Heliyon 5 (2019) e01856

Contents lists available at ScienceDirect

Heliyon

journal homepage: www.heliyon.com

Free vibration of a piezoelectric nanobeam resting on nonlinear Winkler-Pasternak foundation by quadrature methods

Ola Ragb [a], Mokhtar Mohamed [b,*], M.S. Matbuly [a]

[a] Department of Engineering Mathematics and Physics, Faculty of Engineering, Zagazig University, P.O. 44519, Egypt
[b] Basic Science Departement, Faculty of Engineering, Delta University for Science and Technology, P.O.2770141, Egypt

ARTICLE INFO

Keywords:
Applied mathematics
Nonlocal elasticity theory
Vibration
Piezoelectric
Nonlinear elastic foundation
SINC
Discrete singular convolution
Differential quadrature
Open and closed circuit

ABSTRACT

This work introduces a numerical scheme for free vibration analysis of elastically supported piezoelectric nanobeam. Based on Hamilton principle, governing equations of the problem are derived. The problem is formulated for linear and nonlinear Winkler–Pasternak foundation type. Three differential quadrature techniques are employed to reduce the problem to an Eigen-value problem. The reduced system is solved iteratively. The natural frequencies of the beam are obtained. Numerical analysis is implemented to investigate computational characteristics affecting convergence, accuracy and efficiency of the proposed scheme. The obtained results agreed with the previous analytical and numerical ones. Furthermore, a parametric study is introduced to show influence of supporting conditions, two different electrical boundary conditions, material characteristics, foundation parameters, temperature change, external electric voltage, nonlocal parameter and beam length-to-thickness ratio on the values of natural frequencies and mode shapes of the problem.

1. Introduction

A wide range of applications are found concerning elasticity supported piezoelectric nanobeams especially for automobile, aircrafts, electronic, biomedical sectors and several engineering structures [1, 2, 3, 4, 5]. Bending, vibration, and buckling analysis of nanostructures (nanowires, nanoplates, nanorings, nanobeams) play vital role in various engineering applications [6]. Piezoelectric nanostructures found a great attention from research communities [7,8]. Ke et al. [9] investigated linear and nonlinear vibration of piezoelectric nanobeams based on Timoshenko beam theory by using the differential quadrature method. Ebrahimi et al. [10] introduced electromechanical buckling behavior of size-dependent flexoelectric and piezoelectric nanobeams based on nonlocal and surface elasticity theories. Chen et al. [11] developed a micro-scale free vibration analysis of composite laminated Timoshenko beam (CLTB) model based on the new modfied couple stress theory. Shen et al. [12] studied vibration of carbon nanotube (CNT) based on biosensor. A carbon nanotube–based biosensor is modeled as a nonlocal Timoshenko beam. Moreover, Shen et al. [13] explored the potential of single - walled carbon nanotube (SWCNT) as a micro-mass sensor by using transfer function method. Li et al. [14] presented a theoretical treatment of Timoshenko beams, in which the influences of shear deformation, rotary inertia, and scale coefficient are taken into account. Huang et al. [15] analyzed the behavior of flexural waves traveling in carbon nanotubes in free space which are embedded in an elastic matrix. Akgöz et al. [16] proposed higher-order continuum theories for the buckling analysis of single walled carbon nanotubes (SWCNT) by using modified strain gradient elasticity and couple stress theories.

Recently, there are an increasing number of studies on nonlocal theoretical models, which include different kinds of nonlocal elasticity approaches consisting softening and hardening models that are investigated extensively. There are different types of size dependent continuum theory such as micropolar elasticity, couple stress theory, strain gradient elasticity, stress gradient elasticity and surface energy theory. Nonlocal elasticity theory is applied for modeling of nano/micro sized mechanical systems due to its generality and simplicity. Li et al. [17] examined the longitudinal dynamic behaviors of some common one-dimensional nanostructures using the hardening nonlocal approach. Shen et al. [18] developed a modified semi-continuum Euler beam model with relaxation phenomenon and the bending deformation of extreme-thin beam with micro/nano-scale thickness. Mercan et al. [19] applied a discrete singular convolution for buckling behavior of boron nitride nanotube (BNNT), surrounded by an elastic matrix. Due to excellent mechanical, electrical and thermal operations of the nanostructures-with respect to the

* Corresponding author.
E-mail address: mokhtar_husein@yahoo.com (M. Mohamed).

https://doi.org/10.1016/j.heliyon.2019.e01856
Received 20 December 2018; Received in revised form 1 February 2019; Accepted 28 May 2019

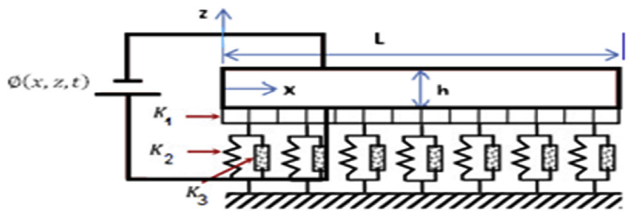

Fig. 1. Piezoelectric nanobeam resting on a nonlinear elastic foundation.

conventional structural materials-they have obtained great interest in the modern science and technology in recent years; such as, micro/nano electromechanical systems [20], nanoresonators [21], chemical sensors [22] and biosensors [12].

Because of the complexity of such problems, only limited cases can be solved analytically [23, 24, 25]. Numerical techniques such as Finite elements [26,27], meshless [28], Galerkin [29], spline finite strip [30], least squares [31] and Rayleigh-Ritz [32] techniques were used to solve such Nano problems. The main drawbacks of such methods are the need for large number of grid points, in addition to a large computational time needed to reach the required accuracy. Lately, a differential quadrature method (DQM) becomes the most popular method in the numerical solutions of boundary value problems [33,34,35,36,37,38]. This method leads to accurate solutions with fewer grid points. The convergence and stability of this method depend on choice of shape function. Lagrange interpolation polynomials, Cardinal sine function, Delta Lagrange Kernel (DLK) and Regularized Shannon kernel (RSK) are some of such functions which lead to polynomial based differential quadrature method (PDQM), Sinc differential quadrature method (SDQM) [39], and Discrete singular convolution differential quadrature method (DSCDQM), respectively [40,41,42,43,44,45,46,47,48,49,50,51].

According to the knowledge of the authors, SDQM and DSCDQM are not examined for vibration analysis of elastically supported piezoelectric nanobeams resting on linear or nonlinear Winkler–Pasternak foundation type. A numerical scheme based on SDQM and DSCDQM is introduced to reduce the problem to reach an Eigen value problem. MATLAB program is designed to solve this problem. The natural frequencies are obtained and compared with previous analytical and numerical ones. For each scheme, the convergence and efficiency are verified. Also, a parametric study is introduced to investigate the influence of supporting conditions, two different electrical boundary conditions, material characteristics, foundation parameters, temperature change, external electric voltage, nonlocal parameter and beam length-to-thickness on the values of natural frequencies and mode shapes of the problem.

2. Theory/Calculation

Consider a piezoelectric nanobeam with ($0 \le x \le L$, $0 \le z \le h$) where L and h are length and thickness of the beam. This beam is polarized in z direction and subjected to an applied voltage$\phi(x,z,t)$, a uniform temperature change ΔT and resting on a nonlinear Winkler-Pasternak foundation K_1 , K_2 and K_3as shown in Fig. (1).

Based on Eringen's nonlocal elasticity theory, the basic equations without body force for a homogeneous nonlocal piezoelectric solid can be written as [9]:

$$\sigma_{ij} = \int_v \alpha(|x' - x|,\ \tau)\left[C_{ijkl}\varepsilon_{kl}(x') - e_{kij}E_k(x') - \lambda_{ij}\Delta T\right] \mathrm{d}x', \tag{1}$$

$$D_i = \int_v \alpha(|x' - x|,\ \tau)\left[e_{ikl}\varepsilon_{kl}(x') - \in_{ik}E_k(x') + p_i\Delta T\right] \mathrm{d}x', \tag{2}$$

$$\sigma_{ij,j} = \rho\ddot{u}_i,\ \mathrm{D}_{i,i} = 0, \tag{3}$$

$$\varepsilon_{ij} = \left(u_{i,j} + u_{j,i}\right)/2,\ \mathrm{E}_i = -\phi_i, \tag{4}$$

Also, the integral constitutive relations represent in differential form as [9,52]:

$$\sigma_{ij} - (e_0a)^2\nabla^2\sigma_{ij} = C_{ijkl}\varepsilon_{kl} - e_{kij}E - \lambda_{ij}\Delta T, \tag{5}$$

$$D_i - (e_0a)^2\nabla^2 D_i = e_{ikl}\varepsilon_{kl} + \in_{ik}E_k + p_i\Delta T, \tag{6}$$

Where D, E, C, e, ρ, ε, σ, p and $\in$ are electric displacement, electric field, elastic constant, piezoelectric constant, mass density, strain, stress electric, pyroelectric constants and dielectric constants. Also, the values of these constants are depending on the type of the material. $\alpha(|x' - x|,\ \tau)$ is the function of nonlocal attenuation. It incorporates into the constitutive equations at the reference point x. $|x' - x|$is the Euclidean distance.

$\nabla^2$is Laplace operator. ($\tau = e_0a/L$)is the scale coefficient revealing the size effect on the response of structures in Nano size ($e_0$is a nondimensional material constant, and a is an internal characteristic length. e_0 can be estimated by experiments or numerical simulations from lattice dynamics [6,19]).

From Fig. (1), the nonlocal constitutive relations (5–6) can be approximated as:

$$\sigma_{xx} = C_{11}\varepsilon_{xx} - e_{31}E_z - \lambda_1\Delta T, \tag{7}$$

$$\sigma_{xz} = C_{44}\gamma_{xz} - e_{15}E_x, \tag{8}$$

$$D_x = e_{15}\gamma_{xz} + \in_{11}E_x, \tag{9}$$

$$D_z = e_{31}\varepsilon_{xx} + \in_{33}E_z + p_1\Delta T, \tag{10}$$

Where $\varepsilon_{xx} = \frac{\partial U}{\partial x}$, $\gamma_{xz} = \frac{\partial W}{\partial x} + \Psi$.

Furthermore, based on Hamilton principle, equations of motion of the problem can be written as [9]:

$$\mathrm{A}_{11}\frac{\partial^2 \mathrm{U}}{\partial x^2} = \mathrm{I}_1\frac{\partial^2}{\partial t^2}\left[\mathrm{U} - (e_0 a)^2\frac{\partial^2 \mathrm{U}}{\partial x^2}\right] \tag{11}$$

$$\mathrm{k_s A_{44}}\left[\frac{\partial^2 \mathrm{W}}{\partial x^2} + \frac{\partial \Psi}{\partial x}\right] - \mathrm{k_s E_{15}}\frac{\partial^2 \phi}{\partial x^2} + (\mathrm{N_E} + \mathrm{N_T})\frac{\partial^2 \mathrm{W}}{\partial x^2} - (\mathrm{N_E} + \mathrm{N_T})(e_0 a)^2\frac{\partial^4 \mathrm{W}}{\partial x^4}$$
$$+ K_1\ W - K_2\frac{\partial^2 \mathrm{W}}{\partial x^2} + K_3\ W^3 = \mathrm{I}_1\frac{\partial^2}{\partial t^2}\left[\mathrm{W} - (e_0 a)^2\frac{\partial^2 \mathrm{W}}{\partial x^2}\right],\ \rightarrow\ (\mathrm{N_T} = -\lambda_1 h\Delta T\ ,$$
$$\mathrm{N_E} = 2e_{31}\mathrm{V}_0) \tag{12}$$

$$\mathrm{D}_{11}\frac{\partial^2 \Psi}{\partial x^2} - \mathrm{k_s A_{44}}\left(\frac{\partial \mathrm{W}}{\partial x} + \Psi\right) + \mathrm{F}_{31}\frac{\partial \phi}{\partial x} + \mathrm{k_s E_{15}}\frac{\partial \phi}{\partial x} = \mathrm{I}_3\frac{\partial^2}{\partial t^2}\left[\Psi - (e_0 a)^2\frac{\partial^2 \Psi}{\partial x^2}\right], \tag{13}$$

$$\mathrm{F}_{31}\frac{\partial \Psi}{\partial x} + \mathrm{E}_{15}\left[\frac{\partial^2 \mathrm{W}}{\partial x^2} + \frac{\partial \Psi}{\partial x}\right] + \mathrm{X}_{11}\frac{\partial^2 \phi}{\partial x^2} - \mathrm{X}_{33}\phi = 0, \tag{14}$$

Where $U(x,t)$, $\mathrm{W}(x,t)$ and $\Psi(x,t)$are longitudinal, lateral displacements and cross section rotation, respectively. t is time. k_s is the shear correction factor which is taken as 5/6 for the macro scale beams [19]. N_T is normal force induced by the temperature change ΔT. N_E is normal force induced by the external electric voltage V_0 . λ_1, e_{31} are thermal module and piezoelectric constant. K_1, K_2 are shear and spring coefficients of linear elastic foundation and $K_3$is a nonlinear elastic foundation [52,53,54,55].

The relation between the constants D, E, C, e, ρ and $\in$ and the values of A_{11}, A_{44}, E_{15}, F_{31}, X_{11}, $\mathrm{X}_{33}$are

The boundary conditions can be described as [9,24,25,60,61]:

(1) For Clamped - Clamped Beam (C–C)

It is assumed that the electric potential is zero [9,24,25,60].

$$(A_{11},\ A_{44})=(C_{11},C_{44})h\ ,D_{11}=\ C_{11}h^3/12\ ,\ \ E_{15}=2\frac{e_{15}}{\beta}\sin\left(\frac{\beta h}{2}\right),\ (I_1,I_3\ )=\rho\left(h,h^3/12\right)\ ,$$
$$F_{31}=\ e_{31}\left[-h\cos\left(\frac{\beta h}{2}\right)+\frac{2}{\beta}\sin\left(\frac{\beta h}{2}\right)\right],X_{11}=\ \frac{\in_{11}}{2}\left[h+\frac{\sin(\beta h)}{\beta}\right],\ \ X_{33}=\ \frac{\in_{33}\beta^2}{2}\left[h-\frac{\sin(\beta h)}{\beta}\right],\beta=\pi/h \tag{15}$$

$$U(0,t)=W(0,t)=\Psi(0,t)=\phi(0,t)=0,\quad U(L,t)=W(L,t)=\Psi(L,t)=\phi(L,t)=0 \tag{16}$$

(2) For Hinged- Hinged Beam (H–H):

$$\begin{aligned}&U(0,t)=W(0,t)=\phi(0,t)=0,\ U(L,t)=W(L,t)=\phi(L,t)=0\\&D_{11}\frac{\partial\Psi(0,t)}{\partial x}+F_{31}\phi(0,t)-\omega^2(e_0a)^2\left[I_3\frac{\partial\Psi(0,t)}{\partial x}+I_1W(0,t)-(e_0a)^2I_1\frac{\partial^2U(0,t)}{\partial x^2}\right]-(N_E+N_T)(e_0a)^2\frac{\partial^2W(0,t)}{\partial x^2}=0,\\&D_{11}\frac{\partial\Psi(L,t)}{\partial x}+F_{31}\phi(L,t)-\omega^2(e_0a)^2\left[I_3\frac{\partial\Psi(L,t)}{\partial x}+I_1W(L,t)-(e_0a)^2I_1\frac{\partial^2U(L,t)}{\partial x^2}\right]-(N_E+N_T)(e_0a)^2\frac{\partial^2W(L,t)}{\partial x^2}=0,\end{aligned} \tag{17}$$

(3) For Clamped - Hinged Beam (C–H):

$$\begin{aligned}&U(0,t)=W(0,t)=\Psi(0,t)=\phi(0,t)=0,\qquad U(L,t)=W(L,t)=\phi(L,t)=0,\\&D_{11}\frac{\partial\Psi(L,t)}{\partial x}+F_{31}\phi(L,t)-\omega^2(e_0a)^2\left[I_3\frac{\partial\Psi(L,t)}{\partial x}+I_1W(L,t)-(e_0a)^2I_1\frac{\partial^2U(L,t)}{\partial x^2}\right]-(N_E+N_T)(e_0a)^2\frac{\partial^2W(L,t)}{\partial x^2}=0,\end{aligned} \tag{18}$$

The electrical potential is different at types of electrical boundary conditions. Therefore, electrical potential can be expressed as:

(1) Closed circuit boundary condition:

$$\phi(0,t)=0,\quad \phi(L,t)=0, \tag{19}$$

(2) Open circuit boundary condition [61]:

$$\begin{aligned}&D_z=0,\ \text{where } D_z\ \textit{is}\ \text{electrical dispacement}\\&\therefore F_{31}\frac{\partial\Psi(0,t)}{\partial x}-X_{33}\ \phi(0,t)=0,\quad F_{31}\frac{\partial\Psi(L,t)}{\partial x}-X_{33}\ \phi(L,t)=0\end{aligned} \tag{20}$$

The field quantities are normalized such as:

$$\begin{aligned}&\zeta=\frac{x}{L},\ w=\frac{W}{h},\ \psi=\Psi,\eta=\frac{L}{h},\ \mu=\frac{e_0a}{L},\ \varphi=\frac{\phi}{\phi_0},\ \phi_0=\sqrt{\frac{\varepsilon_{33}}{A_{11}}},\ \overline{A}_{11}=\frac{A_{11}}{A_{11}}=1,\ \overline{A}_{44}=\frac{A_{44}}{A_{11}},\ \overline{D}_{11}=\frac{D_{11}}{A_{11}h^2},\bar{I}_1=\frac{I_1}{I_1}=1,\bar{I}_3=\frac{I_3}{I_1h^2},\overline{X}_{11}=\frac{X_{11}\phi_0^2}{A_{11}h^2},\\&\overline{X}_{33}=\frac{X_{33}\phi_0^2}{A_{11}},\overline{E}_{15}=\frac{E_{15}\phi_0}{A_{11}h},\overline{F}_{31}=\frac{F_{31}\phi_0}{A_{11}h}\\&\overline{N}_T=-\frac{\lambda h\Delta T}{A_{11}},\ \overline{N}_E=\frac{2e_{31}V_0}{A_{11}},\tau=\frac{t}{L}\sqrt{\frac{I_1}{A_{11}}},\ k_1=\frac{K_1L^4}{\pi^2A_{11}h^2},k_2=\frac{K_2L^2}{\pi^2A_{11}h^2},k_3=\frac{K_3L^2}{\pi^2A_{11}h^2},\end{aligned} \tag{21}$$

Further, for harmonic behavior of the problem, one can assume that:

$$U(x,t)=ue^{i\omega t},\ W(x,t)=we^{i\omega t},\ \Psi(x,t)=\psi e^{i\omega t},\ \phi(x,t)=\varphi e^{i\omega t} \tag{22}$$

where ω.is the dimensionless natural frequency of the beam and $i=\sqrt{-1}$.

u, w, ψ and φ, are the amplitudes of U, W, $\Psi and \phi$ respectively.

Substituting from Eqs. (21) and (22) into (11, 12, 13, 14), the problem can be reduced to a quasi-static one as:

$$\frac{\partial^2 u}{\partial\zeta^2}=-\omega^2\left[u-\mu^2\frac{\partial^2 u}{\partial\zeta^2}\right], \tag{23}$$

$$\mathrm{k_s}\overline{\mathrm{A}}_{44}\left[\frac{\partial^2 w}{\partial\zeta^2}+\eta\frac{\partial\psi}{\partial\zeta}\right]-\mathrm{k_s}\overline{\mathrm{E}}_{15}\frac{\partial^2\varphi}{\partial\zeta^2}+(\overline{\mathrm{N}}_\mathrm{E}+\overline{\mathrm{N}}_\mathrm{T})\frac{\partial^2 w}{\partial\zeta^2}-(\overline{\mathrm{N}}_\mathrm{E}+\overline{\mathrm{N}}_\mathrm{T})\mu^2\frac{\partial^4 w}{\partial\zeta^4}+$$
$$k_1 w-k_2\frac{\partial^2 w}{\partial\zeta^2}+k_3 w^3=-\omega^2\left[w-\mu^2\frac{\partial^2 w}{\partial\zeta^2}\right], \tag{24}$$

$$\overline{\mathrm{D}}_{11}\frac{\partial^2\psi}{\partial\zeta^2}-\mathrm{k_s}\overline{\mathrm{A}}_{44}\eta\left(\frac{\partial w}{\partial\zeta}+\eta\psi\right)+(\overline{\mathrm{F}}_{31}+\mathrm{k_s}\overline{\mathrm{E}}_{15})\eta\frac{\partial\varphi}{\partial\zeta}=-\omega^2\bar{\mathrm{I}}_3\left[\psi-\mu^2\frac{\partial^2\varphi}{\partial\zeta^2}\right], \tag{25}$$

$$\overline{\mathrm{F}}_{31}\eta\frac{\partial\psi}{\partial\zeta}+\overline{\mathrm{E}}_{15}\left[\frac{\partial^2 w}{\partial\zeta^2}+\eta\frac{\partial\psi}{\partial\zeta}\right]+\overline{\mathrm{X}}_{11}\frac{\partial^2\varphi}{\partial\zeta^2}-\overline{\mathrm{X}}_{33}\eta^2\varphi=0 \tag{26}$$

Also, the boundary conditions (16–20) can be rewritten as:

(1) For Clamped - Clamped Beam (C–C)

$$u=w=\psi=\varphi=0\ \zeta=0,\ 1 \tag{27}$$

(2) For Hinged- Hinged Beam (H–H):

$$u=w=\varphi=0$$
$$\zeta=0,\ 1$$
$$\overline{\mathrm{D}}_{11}\frac{\partial\psi}{\partial\zeta}+\overline{\mathrm{F}}_{31}\eta\varphi-\omega^2\mu^2\left[\bar{\mathrm{I}}_3\frac{\partial\psi}{\partial\zeta}+\eta\mathrm{w}-\mu^2\eta\frac{\partial^2 u}{\partial\zeta^2}\right]-\eta(\overline{\mathrm{N}}_\mathrm{E}+\overline{\mathrm{N}}_\mathrm{T})\mu^2\frac{\partial^2 w}{\partial\zeta^2}=0 \tag{28}$$

(3) For Clamped - Hinged Beam (C–H):

$$u=w=\psi=\varphi=0,\ \zeta=0$$
$$u=w=\varphi=0\qquad \zeta=1$$
$$\overline{\mathrm{D}}_{11}\frac{\partial\psi}{\partial\zeta}+\overline{\mathrm{F}}_{31}\eta\varphi-\omega^2\mu^2\left[\bar{\mathrm{I}}_3\frac{\partial\psi}{\partial\zeta}+\eta\mathrm{w}-\mu^2\eta\frac{\partial^2 u}{\partial\zeta^2}\right]-\eta(\overline{\mathrm{N}}_\mathrm{E}+\overline{\mathrm{N}}_\mathrm{T})\mu^2\frac{\partial^2 w}{\partial\zeta^2}=0, \tag{29}$$

For closed circuit:

$$\varphi=0\ \zeta=0,1 \tag{30}$$

For open circuit

$$\overline{F}_{31}\eta\frac{\partial\psi}{\partial\zeta}-\overline{X}_{33}\eta^2\varphi=0,\ \zeta=0,1 \tag{31}$$

3. Methodology

Three differential quadrature techniques are employed to reduce the problem to an eigen value one as follows [33,34,35,36,37,38].

- Polynomial based differential quadrature method (PDQM)

In this technique, Lagrange interpolation polynomial is employed as a shape function such that the unknown v and its n^{th} derivatives can be approximated as a weighted linear sum of nodal values, v_i ($i=1:N$), as follows [56]:

$$v(x_i)=\sum_{j=1}^{N}\frac{\prod_{k=1}^{N}(x_i-x_k)}{(x_i-x_j)\prod_{j=1,j\neq k}^{N}(x_j-x_k)}v(x_j),(i=1:N), \tag{32}$$

$$\left.\frac{\partial^n v}{\partial x^n}\right|_{x=x_i}=\sum_{j=1}^{N}C_{ij}^{(n)}v(x_j)\ (i=1:N) \tag{33}$$

Where v terms to the field quantities u, w,ψ and φ. N is the number of grid points. The weighting coefficients of the first order derivative$C_{ij}^{(1)}$ can be determined as [56]:

$$C_{ij}^{(1)}=\begin{cases}\dfrac{1}{(x_i-x_j)}\displaystyle\prod_{k=1,k\neq i,j}^{N}\frac{(x_i-x_k)}{(x_j-x_k)}\ i\neq j\\[2ex] -\displaystyle\sum_{j=1,j\neq i}^{N}C_{ij}^{(1)}\ i=j\end{cases} \tag{34}$$

By using matrix multiplication, the weighting coefficients of higher order derivatives, can be calculated as:

$$\left[C_{ij}^{(n)}\right]=\left[C_{ij}^{(1)}\right]\left[C_{ij}^{(n-1)}\right],(n=2,3,4) \tag{35}$$

- Sinc Differential Quadrature Method (SDQM)

In this method, cardinal sine function is used as a shape function such that the unknown v and its derivatives can be approximated as a weighted linear sum of nodal values, vi (i = –N: N), as follows [39]:

$$S_j(x_i,h_x)=\frac{\sin\left[\pi(x_i-x_j)/h_x\right]}{\pi(x_i-x_j)/h_x},\ \text{Where }(\mathrm{hx}>0)\text{ is the step size.} \tag{36}$$

$$v(x_i)=\sum_{j=-N}^{N}\frac{\sin\left[\pi(x_i-x_j)/h_x\right]}{\pi(x_i-x_j)/h_x}v(x_j),\ (i=-N:N),h_x>0 \tag{37}$$

$$\frac{\partial v}{\partial x}|x=x_i=\sum_{j=-N}^{N}C_{ij}^{(1)}v(x_j),\ \frac{\partial^2 v}{\partial x^2}|x=x_i=\sum_{j=-N}^{N}C_{ij}^{(2)}v(x_j),$$
$$\frac{\partial^3 v}{\partial x^3}|x=x_i=\sum_{j=-N}^{N}C_{ij}^{(3)}v(x_j),\ \frac{\partial^4 v}{\partial x^4}|x=x_i=\sum_{j=-N}^{N}C_{ij}^{(4)}v(x_j),\ (i=-N:N), \tag{38}$$

where v terms to the field quantities. N is the number of grid points. h_x is grid size. The weighting coefficients$C_{ij}^{(1)}$, $C_{ij}^{(2)}$,$C_{ij}^{(3)}$ *and* $C_{ij}^{(4)}$ can be determined by differentiating (36) and (37) as:

$$C_{ij}^{(1)} = \begin{cases} \dfrac{(-1)^{i-j}}{h_x(i-j)}, & i \neq j \\ 0 & i = j \end{cases}, C_{ij}^{(2)} = \begin{cases} \dfrac{2(-1)^{i-j+1}}{h_x^2(i-j)^2}, & i \neq j \\ -\dfrac{\pi^2}{3h_x^2} & i = j \end{cases}$$

$$C_{ij}^{(3)} = \begin{cases} \dfrac{(-1)^{i-j}}{h_x^3(i-j)^3}\left(6-\pi^2(i-j)^2\right), & i \neq j \\ 0 & i = j \end{cases}, C_{ij}^{(4)} = \begin{cases} \dfrac{4(-1)^{i-j+1}}{h_x^4(i-j)^4}\left(6-\pi^2(i-j)^2\right), & i \neq j \\ \dfrac{\pi^4}{5h_x^4} & i = j \end{cases} \quad (39)$$

- Discrete Singular Convolution Differential Quadrature Method (DSCDQM)

Based on singular convolution defined as [40, 41, 42, 43, 44, 45, 46, 47, 48,49, 50, 51].

$$F(t) = (T * \eta)(t) = \int_{-\infty}^{\infty} T(t-x)\eta(x)dx \quad (40)$$

Where $T(t-x)$is a singular kernel.

The DSC algorithm can be applied using many types of kernels. These kernels are applied as shape functions such that the unknown v and its derivatives are approximated as a weighted linear sum of v_i (i= -N: N), over a narrow bandwidth ($x-x_M$,$x+x_M$) [40, 41, 42, 43, 44, 45, 46, 47, 48, 49, 50, 51].

Two kernels of DSC will be employed as follows:

(a) Delta Lagrange Kernel (DLK) can be used as a shape function such that the unknown v and its derivatives can be approximated as follows:

$$v(x_i) = \sum_{j=-M}^{M} \frac{\prod_{k=-M}^{M}(x_i - x_k)}{(x_i - x_j)\prod_{j=-M, j\neq k}^{M}(x_j - x_k)} v(x_j), \ (i = -N:N), M \geq 1 \quad (41)$$

$$\frac{\partial v}{\partial x}|x = x_i = \sum_{j=-M}^{M} C_{ij}^{(1)} v(x_j), \frac{\partial^2 v}{\partial x^2}|x = x_i = \sum_{j=-M}^{M} C_{ij}^{(2)} v(x_j),$$
$$\frac{\partial^3 v}{\partial x^3}|x = x_i = \sum_{j=-M}^{M} C_{ij}^{(3)} v(x_j), \frac{\partial^4 v}{\partial x^4}|x = x_i = \sum_{j=-M}^{M} C_{ij}^{(4)} v(x_j), (i = -N:N), \quad (42)$$

where 2M + 1 is the effective computational band width.

$C_{ij}^{(1)}$, $C_{ij}^{(2)}$, $C_{ij}^{(3)}$ *and* $C_{ij}^{(4)}$ *are defined as* :

$$C_{ij}^{(1)} = \begin{cases} \dfrac{1}{(x_i - x_j)} \prod_{k=-M, k\neq i,j}^{M} \dfrac{(x_i - x_k)}{(x_j - x_k)} \ i \neq j \\ -\sum_{j=-M, j\neq i}^{M} C_{ij}^{(1)} \ i = j \end{cases}, C_{ij}^{(2)} = \begin{cases} 2\left(C_{ij}^{(1)} C_{ii}^{(1)} - \dfrac{C_{ij}^{(1)}}{(x_i - x_j)}\right) i \neq j \\ -\sum_{j=-M, j\neq i}^{M} C_{ij}^{(2)} \ i = j \end{cases}, \quad (43)$$

$$C_{ij}^{(3)} = \begin{cases} 3\left(C_{ij}^{(1)} C_{ii}^{(2)} - \dfrac{C_{ij}^{(2)}}{(x_i - x_j)}\right) i \neq j \\ -\sum_{j=-M, j\neq i}^{M} C_{ij}^{(3)} \ i = j \end{cases}, C_{ij}^{(4)} = \begin{cases} 4\left(C_{ij}^{(1)} C_{ii}^{(3)} - \dfrac{C_{ij}^{(3)}}{(x_i - x_j)}\right) i \neq j \\ -\sum_{j=-M, j\neq i}^{M} C_{ij}^{(4)} \ i = j \end{cases}, \quad (44)$$

(b) Regularized Shannon kernel (RSK) can also be used as a shape function such that the unknown v and its derivatives can be approximated as follows:

$$\psi(x_i) = \sum_{j=-M}^{M} \left\langle \frac{\sin[\pi(x_i - x_j)/h_x]}{\pi(x_i - x_j)/h_x} e^{-\left(\frac{(x_i - x_j)^2}{2\sigma^2}\right)} \right\rangle \psi(x_j), (i = -N : N), \sigma = (r * h_x) > 0 \quad (45)$$

Table 1
Material property of elasticity supported piezoelectric nanobeam [58,59].

Material properties	Elastic Constant (GPa)		Piezoelectric Constant (C/m^2)		Dielectric Constants (C/Vm) *10^{-9}		Thermal module (N/m^{2}K) *10^5	Density (kg/m^3)
	C_{11}	C_{44}	e_{31}	e_{15}	ε_{11}	ε_{33}	λ_1	P
PZT-4	132	26	-4.1	14.1	5.841	7.124	4.738	7500
BiTiO3–COFe2O4	226	44.2	-2.2	5.8	5.64	6.35	4.74	5550

Table 2
Comparison between the obtained normalized frequencies, due to PDQM, grid sizes and the previous exact and numerical ones, for clamped hinged nanobeam. ($V_0 = 0$, $\Delta T = 0$, $L = 12nm$, $\mathrm{h} = 2\mathrm{nm}$, $\mu = 0$, $\mathrm{k}_1 = \mathrm{k}_2 = \mathrm{k}_3 = 0$)

Normalized frequencies / Grid size N	ω_1	ω_2	ω_3	ω_4	ω_5
3	1.14592	2.8283	8.6761	---------	---------
5	0.6319	2.17824	3.1343	3.4421	6.9282
7	0.6323	1.7963	3.1416	3.4638	5.0183
9	0.6323	1.70999	2.94503	3.1416	4.2833
11	0.6323	1.740	3.1416	3.3040	3.8070
Exact results [60]	0.6323	-----------	-----------	---------	---------
PDQM [9] N = 15	0.6323	-----------	-----------	---------	---------
Execution time (sec)	0.158375– over 7 non-uniform grid				

Table 3
Comparison between the obtained normalized frequencies, due to SINC DQM, grid sizes and the previous exact and numerical ones for clamped hinged nano beam. ($V_0 = 0$, $\Delta T = 0$, $L = 12nm$, $\mathrm{h} = 2\mathrm{nm}$, $\mu = 0$, $\mathrm{k}_1 = \mathrm{k}_2 = \mathrm{k}_3 = 0$)

Normalized frequencies / Grid size N	ω_1	ω_2	ω_3	ω_4	ω_5
3	1.2184	2.9554	8.9921	-----------	-----------
5	0.6255	1.5142	2.5907	3.0267	5.17044
7	0.6294	1.4906	2.5866	2.6281	3.803
9	0.6323	1.49676	2.5857	2.64027	3.8051
11	0.6323	1.49826	2.5856	2.64151	3.8095
Exact results [60]	0.6323	-----------	---------	-----------	-----------
PDQM [9] N = 15	0.6323	-----------	---------	-----------	-----------
Execution time (sec)	0.142314– over 9 uniform grid				

Table 4
Comparison between the normalized fundamental frequency by using DSCDQM-DLK, band width (2M + 1) and grid size N for clamped hinged nanobeam. ($V_0 = 0$, $\Delta T = 0$, $L = 12nm$, $\mathrm{h} = 2\mathrm{nm}$, $\mu = 0$, $\mathrm{k}_1 = \mathrm{k}_2 = \mathrm{k}_3 = 0$)

Fundamental frequency	DSCDQM-DLK				
Band width / N	3	5	7	9	11
2M + 1 = 3	0.6323	0.6323	0.6323	0.6323	0.6323
2M + 1 = 5	0.6323	0.6323	0.6323	0.6323	0.6323
2M + 1 = 7	0.6323	0.6323	0.6323	0.6323	0.6323
2M + 1 = 9	0.6323	0.6323	0.6323	0.6323	0.6323
2M + 1 = 11	0.6323	0.6323	0.6323	0.6323	0.6323
Execution time (sec)	0.1400– over 3 uniform grid				

Table 5
Comparison between the obtained normalized frequencies, due to DSCDQM-DLK, grid sizes and the previous exact and numerical ones, for clamped hinged nanobeam. ($V_0 = 0$, $\Delta T = 0$, $L = 12nm$, $\mathrm{h} = 2\mathrm{nm}$, $\mu = 0$, $2\mathrm{M}+1 = 3$, $\mathrm{k}_1 = \mathrm{k}_2 = \mathrm{k}_3 = 0$)

Normalized frequencies / Grid size N	ω_1	ω_2	ω_3	ω_4	ω_5
3	0.6323	1.556178	3.121593	3.12533	4.38459
5	0.6323	1.556178	3.121593	3.12533	4.38459
7	0.6323	1.556178	3.121593	3.12533	4.38459
9	0.6323	1.556178	3.121593	3.12533	4.38459
Exact results [60]	0.6323	-------------	-------------	-----------	-----------
PDQM [9] N = 15	0.6323	-------------	-------------	-----------	-----------
Execution time (sec)	0.1400– over 3 uniform grid				

Table 6
Comparison between the normalized fundamental frequency by using DSCDQM-RSK, band width (2M + 1) regularization parameter σ and grid size N for clamped hinged nano elastic beam. ($V_0 = 0,\ \Delta T = 0,\ L = 12nm$, h = 2nm, $\mu = 0$, $k_1 = k_2 = k_3 = 0$)

fundamental frequency	regularization parameter	DSCDQM-RSK				
N	2M + 1	σ = 1*h_x	σ = 1.5*h_x	σ = 1.8*h_x	σ = 1.95*h_x	σ = 2*h_x
3	3	1.22835	0.81413	0.67747	0.63488	0.6323
	5	1.22835	0.81413	0.67747	0.63488	0.6323
	7	1.22835	0.81413	0.67747	0.63488	0.6323
5	3	1.22835	0.81413	0.67747	0.63488	0.6323
	5	1.22835	0.81413	0.67747	0.63488	0.6323
	7	1.22835	0.81413	0.67747	0.63488	0.6323
7	3	1.22835	0.81413	0.67747	0.63488	0.6323
	5	1.22835	0.81413	0.67747	0.63488	0.6323
	7	1.22835	0.81413	0.67747	0.63488	0.6323
9	3	1.22835	0.81413	0.67747	0.63488	0.6323
	5	1.22835	0.81413	0.67747	0.63488	0.6323
	7	1.22835	0.81413	0.67747	0.63488	0.6323

Table 7
Comparison between the obtained normalized frequencies, due to DSCDQM-RSK, grid sizes and the previous exact and numerical ones for clamped hinged nanobeam. ($V_0 = 0,\ \Delta T = 0,\ L = 12nm$, h = 2nm, $\mu = 0$, 2M+ 1 = 3, $k_1 = k_2 = k_3 = 0$)

Normalized frequencies	ω_1	ω_2	ω_3	ω_4	ω_5
Grid size N					
3	0.6323	1.556178	3.121593	3.12533	4.38459
5	0.6323	1.556178	3.121593	3.12533	4.38459
7	0.6323	1.556178	3.121593	3.12533	4.38459
9	0.6323	1.556178	3.121593	3.12533	4.38459
Exact results [60]	0.6323	------------	------------	----------	----------
PDQM [9] N = 15	0.6323	------------	------------	----------	----------
Execution time (sec)	0.139032– over 3 uniform grid				

Table 8
Comparison between the normalized frequencies, linear elastic foundation parameters and the previous numerical ones for clamped piezoelectric nanobeam. ($V_0 = 0$, $\Delta T = 0$, L = 10nm, $L/h = 5$, $k_3 = 0$)

Normalized frequencies			ω_1		ω_2		ω_3	
Elastic foundation parameters		Results	DSCDQM-RSK	PDQM [22]	DSCDQM-RSK	PDQM [22]	DSCDQM-RSK	PDQM [22]
k_2	k_1							
0	0		79.5849	79.5849	158.9145	158.915	226.9817	226.982
	5		79.6553	79.6553	158.9489	158.949	227.0057	227.006
	10		79.7256	79.7256	158.9833	158.983	227.0296	227.03
	15		79.7958	79.7958	159.0177	159.018	227.0535	227.054
	25		79.9361	79.9361	159.0864	159.086	227.1013	227.101
0.025	0		79.6294	79.6294	158.9935	158.994	227.0983	227.098
	5		79.7552	———	159.1307	————	227.474	———
	10		79.8126	————	159.1588	————	2.27493	————
	15		79.86996	————	159.1869	————	227.5126	————
	25		79.9845	————	159.243	————	227.5516	———
0.05	0		79.6738	79.6738	159.0725	159.073	227.2149	227.215
	5		79.8676	———	159.3305	———	227.7683	———
	10		79.92493	———	159.3585	———	227.7878	———
	15		79.98219	———	159.3866	———	227.8072	———
	25		80.0966	———	159.4426	———	227.8462	———
0.1	0		79.7627	79.7627	159.2303	159.2303	227.4478	227.448
	5		80.03462	———	159.789	———	228.398	———
	10		80.2141	———	159.877	———	228.45897	———
	15		80.39327	———	159.9645	———	228.51999	———
	25		80.572002	———	160.1398	———	228.64195	———
0.15	0		79.8514	79.8514	159.3879	159.3879	227.6805	227.6805
	5		80.258170	———	160.18625	———	228.9842	———
	10		80.4372	———	160.2738	———	229.045	———
	15		80.61584	———	1.60.3613	———	229.1059	———
	25		80.794074	———	160.536	———	229.22756	———

Table 9
Comparison between the normalized frequencies and nonlinear elastic foundations for clamped piezoelectric nano beam. ($V_0 = 0$, $\Delta T = 0$, $L = 10nm$, $L/h = 5$)

Nonlinear elastic parameters k_3		0.025		0.05		0.1		0.15	
Linear elastic parameters		Normalized frequencies							
k_2	k_1	ω_1	ω_2	ω_1	ω_2	ω_1	ω_2	ω_1	ω_2
0	0	79.5923	158.905	79.600	158.908	79.614	158.914	79.628	158.919
	5	79.6498	158.933	79.657	158.936	79.672	158.942	79.686	158.947
	10	79.7073	158.962	79.715	158.964	79.729	158.97	79.744	158.976
	15	79.7648	158.99	79.772	158.992	79.787	158.998	79.801	159.004
	25	79.8795	159.046	79.887	159.049	79.901	159.054	79.916	159.06
0.025	0	79.7050	159.105	79.712	159.108	79.727	159.114	79.741	159.119
	5	79.7625	159.133	79.77	159.136	79.784	159.142	79.799	159.148
	10	79.82	159.162	79.827	159.164	79.842	159.17	79.856	159.176
	15	79.877	159.19	79.884	159.192	79.899	159.198	79.913	159.204
	25	79.9918	159.246	79.999	159.248	80.014	159.254	80.028	159.26
0.05	0	79.8175	159.305	79.825	159.308	79.839	159.314	79.854	159.319
	5	79.8749	159.333	79.882	159.336	79.897	159.342	79.911	159.347
	10	79.9322	159.361	79.939	159.364	79.954	159.37	79.968	159.375
	15	79.9894	159.389	79.997	159.392	80.011	159.398	80.026	159.403
	25	80.1039	159.445	80.111	159.448	80.126	159.454	80.140	159.459
0.1	0	80.0419	159.704	80.049	159.707	80.064	159.712	80.078	159.718
	5	80.0991	159.732	80.106	159.735	80.121	159.740	80.135	159.746
	10	80.1562	159.76	80.164	159.763	80.178	159.768	80.193	159.774
	15	80.2133	159.788	80.221	159.791	80.235	159.796	80.25	159.802
	25	80.3275	159.844	80.335	159.847	80.349	159.852	80.364	159.858
0.15	0	80.2655	160.102	80.273	160.104	80.287	160.110	80.302	160.116
	5	80.3225	160.129	80.33	160.132	80.344	160.138	80.359	160.14
	10	80.3795	160.157	80.387	160.160	80.401	160.166	80.416	160.17
	15	80.4364	160.185	80.444	160.188	80.458	160.194	80.473	160.2
	25	80.5502	160.241	80.558	160.244	80.572	160.249	80.587	160.255

Table 10
Comparison between the normalized frequencies, boundary conditions and nonlocal parameter (μ) for piezoelectric nano beam. ($V_0 = 0$, $\Delta T = 0$, L/h = 20, $k_1 = 10$, $k_2 = 0.025$, $k_3 = 0.05$)

Normalized frequencies		ω_1	ω_2	ω_3	ω_4	ω_5
B.C	μ					
CH	0	0.2313	0.6106	1.2897	2.1710	3.1416
	0.05	0.2297	0.5945	1.1927	1.8826	2.5910
	0.1	0.2252	0.5591	1.0238	1.4843	1.9070
	0.15	0.2191	0.5240	0.8949	1.2324	1.5277
	0.2	0.2123	0.4969	0.8125	1.0817	1.3042
	0.5	0.1847	0.4393	0.6678	0.8214	0.8539
	1	0.1722	0.4267	0.6277	0.7854	0.8054
CC	0	0.3205	0.7661	1.4817	2.3799	3.2423
	0.05	0.3204	0.7435	1.3658	2.0581	2.7543
	0.1	0.3202	0.6944	1.1673	1.6177	2.0173
	0.15	0.3199	0.6461	1.0194	1.3391	1.6029
	0.2	0.3197	0.6090	0.9275	1.1689	1.3592
	0.5	0.3187	0.5305	0.8145	0.8311	0.8698
	1	0.3184	0.5148	0.7636	0.8084	0.8269
HH	0	0.1790	0.4610	1.0997	1.9596	2.9905
	0.05	0.1760	0.4500	1.0207	1.7046	2.4195
	0.1	0.1676	0.4255	0.8807	1.3477	1.7790
	0.15	0.1552	0.4002	0.7712	1.1199	1.4231
	0.2	0.1402	0.3800	0.6998	0.9843	1.2181
	0.5	0.0310	0.3339	0.5734	0.7244	0.8382
	1	0.0267	0.3226	0.5512	0.6488	0.7623

Table 11
Comparison between the normalized frequencies, boundary conditions and length-to-thickness ratio (L/h) for piezoelectric nano beam. ($V_0 = 0$, $\Delta T = 0$, h = 2nm, $\mu = 0.1$, $k_1 = 10$, $k_2 = 0.025$, $k_3 = 0.05$)

Normalized frequencies		ω_1	ω_2	ω_3	ω_4	ω_5
B.C	L/h					
CC	6	0.7975	1.6232	2.4590	2.7195	3.2130
	8	0.6580	1.3940	2.1094	2.4276	2.7494
	12	0.4799	1.0624	1.6649	2.1452	2.4886
	16	0.3794	0.8443	1.3693	1.8416	2.2348
	20	0.3202	0.6944	1.1673	1.6177	2.0173
	30	0.2577	0.4676	0.9120	1.3612	1.7823
CH	6	0.6060	1.4753	2.4002	2.4801	2.9972
	8	0.4846	1.2320	1.9710	2.4007	2.6191
	12	0.3431	0.9055	1.5182	2.0440	2.4327
	16	0.2684	0.7009	1.2239	1.7157	2.1409
	20	0.2252	0.5591	1.0238	1.4843	1.9070
	30	0.1485	0.3228	0.7490	1.2063	1.6522
HH	6	0.4282	1.3095	2.2075	2.4697	2.5604
	8	0.3318	1.0587	1.8285	2.3477	2.4303
	12	0.2319	0.7479	1.3669	1.9252	2.3619
	16	0.1868	0.5603	1.0775	1.5828	2.0278
	20	0.1676	0.4255	0.8807	1.3477	1.7790
	30	0.1309	0.1725	0.5791	1.0492	1.4926

Table 12
Comparison between the normalized frequencies and nonlinear elastic foundations for short circuit clamped-Hinged piezoelectric nano beam. ($V_0 = 0$, $\Delta T = 0$, L = 12nm, $L/h = 6$, $\mu = 0.1$)

Nonlinear elastic parameters k_3		0.025		0.05		0.1		0.15	
Linear elastic parameters		Normalized frequencies							
k_2	k_1	ω_1	ω_2	ω_1	ω_2	ω_1	ω_2	ω_1	ω_2
0	0	0.6007	1.4674	0.6007	1.4675	0.6008	1.4675	0.6010	1.4675
	5	0.6025	1.4682	0.6026	1.4682	0.6027	1.4682	0.6028	1.4683
	10	0.6044	1.4689	0.6044	1.4689	0.6046	1.4690	0.6048	1.4691
	15	0.6062	1.4697	0.6063	1.4697	0.6064	1.4697	0.6065	1.4698
	25	0.6099	1.4712	0.6100	1.4712	0.6101	1.4712	0.6102	1.4713
0.025	0	0.6040	1.4724	0.6040	1.4724	0.6042	1.4724	0.6043	1.4725
	5	0.6058	1.4731	0.6059	1.4731	0.6060	1.4732	0.6061	1.4733
	10	0.6077	1.4739	0.6077	1.4739	0.6078	1.4739	0.6079	1.4741
	15	0.6095	1.4746	0.6096	1.4746	0.6097	1.4747	0.6098	1.4749
	25	0.6132	1.4761	0.6132	1.4761	0.6133	1.4762	0.6134	1.4764
0.05	0	0.6073	1.4773	0.6073	1.4773	0.6074	1.4773	0.6076	1.4774
	5	0.6091	1.4780	0.6092	1.4781	0.6093	1.4781	0.6095	1.4783
	10	0.6109	1.4788	0.6110	1.4788	0.6111	1.4788	0.6113	1.4790
	15	0.6128	1.4795	0.6128	1.4795	0.6129	1.4796	0.6131	1.4798
	25	0.6164	1.4810	0.6165	1.4810	0.6166	1.4811	0.6167	1.4812
0.1	0	0.6138	1.4871	0.6138	1.4871	0.6140	1.4871	0.6142	1.4873
	5	0.6156	1.4878	0.6157	1.4879	0.6158	1.4879	0.6160	1.4881
	10	0.6174	1.4886	0.6175	1.4887	0.6176	1.4886	0.6178	1.4888
	15	0.6192	1.4893	0.6193	1.4894	0.6194	1.4893	0.6196	1.4895
	25	0.6228	1.4908	0.6229	1.4909	0.6230	1.4910	0.6232	1.4912
0.15	0	0.6202	1.4968	0.6203	1.4969	0.6204	1.4971	0.6206	1.4973
	5	0.6220	1.4975	0.6221	1.4976	0.6222	1.4977	0.6224	1.4979
	10	0.6238	1.4983	0.6239	1.4984	0.6240	1.4985	0.6241	1.4987
	15	0.6256	1.4990	0.6257	1.4991	0.6258	1.4992	0.6259	1.4994
	25	0.6292	1.5005	0.6293	1.5006	0.6294	1.5007	0.6296	1.5008

Table 13
Comparison between the normalized frequencies and nonlinear elastic foundations for open circuit clamped-Hinged piezoelectric nano beam. ($V_0 = 0$, $\Delta T = 0$, L = 12nm, $L/h = 6$, $\mu = 0.1$)

Nonlinear elastic parameters k_3		0.025		0.05		0.1		0.15	
Linear elastic parameters		Normalized frequencies							
k_2	k_1	ω_1	ω_2	ω_1	ω_2	ω_1	ω_2	ω_1	ω_2
0	0	0.6562	2.1754	0.6563	2.1755	0.6564	2.1756	0.6565	2.1757
	5	0.6579	2.1759	0.6580	2.1760	0.6582	2.1761	0.6582	2.1762
	10	0.6596	2.1765	0.6597	2.1766	0.6598	2.1767	0.6599	2.1768
	15	0.6613	2.1770	0.6614	2.1771	0.6615	2.1772	0.6617	2.1773
	25	0.6647	2.1780	0.6648	2.1781	0.6649	2.1782	0.6650	2.1783
0.025	0	0.6593	2.1829	0.6595	2.1831	0.6596	2.1832	0.6598	2.1833
	5	0.6610	2.1834	0.6611	2.1836	0.6612	2.1838	0.6613	2.1840
	10	0.6627	2.1839	0.6628	2.1841	0.6630	2.1842	0.6632	2.1843
	15	0.6644	2.1844	0.6645	2.1846	0.6646	2.1847	0.6647	2.1848
	25	0.6677	2.1854	0.6679	2.1856	0.6680	2.1857	0.6681	2.1858
0.05	0	0.6624	2.1903	0.6625	2.1905	0.6626	2.1906	0.6627	2.1908
	5	0.6641	2.1908	0.6643	2.1909	0.6645	2.1910	0.6646	2.1912
	10	0.6658	2.1913	0.6660	2.1915	0.6662	2.1916	0.6664	2.1918
	15	0.6675	2.1918	0.6677	2.1919	0.6678	2.1920	0.6680	2.1922
	25	0.6708	2.1928	0.6710	2.1929	0.6711	2.1930	0.6713	2.1931
0.1	0	0.6686	2.2050	0.6688	2.2051	0.6689	2.2052	0.6690	2.2054
	5	0.6702	2.2055	0.6704	2.2056	0.6706	2.2058	0.6708	2.2060
	10	0.6719	2.2060	0.6720	2.2061	0.6722	2.2063	0.6724	2.2065
	15	0.6736	2.2065	0.6737	2.2066	0.6738	2.2068	0.6740	2.2070
	25	0.6769	2.2075	0.6770	2.2076	0.6771	2.2078	0.6772	2.2080
0.15	0	0.6746	2.2197	0.6747	2.2198	0.6748	2.2200	0.6750	2.2202
	5	0.6763	2.2202	0.6764	2.2203	0.6765	2.2205	0.6767	2.2207
	10	0.6780	2.2207	0.6781	2.2208	0.6782	2.2210	0.6783	2.2212
	15	0.6796	2.2211	0.6797	2.2212	0.6798	2.2214	0.6798	2.2215
	25	0.6829	2.2221	0.6830	2.2222	0.6832	2.2224	0.6834	2.2225

Table 14
Comparison between the normalized fundamental frequency and nonlinear elastic foundations for Hinged-Hinged piezoelectric nano beam at two different electrical boundary conditions. ($V_0 = 0$, $\Delta T = 0$, L = 12nm, $L/h = 6$, $\mu = 0.1$).

Nonlinear elastic parameters k_3		0.025		0.05		0.1		0.15	
Linear elastic parameters		Fundamental frequencies							
k_2	k_1	Open circuit	Short circuit	Open circuit	Short circuit	Open circuit	Short circuit	Open circuit	Short circuit
0	0	0.5373	0.4264	0.5374	0.4264	0.5376	0.4265	0.5379	0.4266
	5	0.5394	0.4275	0.5395	0.4276	0.5396	0.4277	0.5399	0.4278
	10	0.5414	0.4286	0.5415	0.4286	0.5416	0.4287	0.5419	0.4288
	15	0.5435	0.4312	0.5436	0.4313	0.5438	0.4315	0.5439	0.4316
	25	0.5476	0.4363	0.5477	0.4363	0.5479	0.4365	0.5482	0.4366
0.025	0	0.5407	0.4273	0.5408	0.4273	0.5410	0.4275	0.5412	0.4276
	5	0.5427	0.4300	0.5428	0.4302	0.5430	0.4303	0.5432	0.4304
	10	0.5448	0.4325	0.5449	0.4326	0.5450	0.4327	0.5452	0.4328
	15	0.5468	0.4351	0.5469	0.4352	0.5471	0.4354	0.5472	0.4355
	25	0.5509	0.4402	0.5510	0.4403	0.5512	0.4405	0.5514	0.4407
0.05	0	0.5440	0.4313	0.5441	0.4314	0.5444	0.4316	0.5446	0.4318
	5	0.5461	0.4339	0.5462	0.4340	0.5465	0.4342	0.5465	0.4345
	10	0.5481	0.4365	0.5482	0.4366	0.5484	0.4369	0.5485	0.4372
	15	0.5502	0.4390	0.5503	0.4392	0.5504	0.4395	0.5505	0.4397
	25	0.5542	0.4441	0.5543	0.4443	0.5544	0.4445	0.5545	0.4448
0.1	0	0.5507	0.4392	0.5508	0.4394	0.5509	0.4395	0.5512	0.4399
	5	0.5527	0.4417	0.5528	0.4419	0.5529	0.4421	0.5531	0.4425
	10	0.5547	0.4442	0.5548	0.4443	0.5549	0.4445	0.5552	0.4446
	15	0.5567	0.4468	0.5568	0.4469	0.5569	0.4472	0.5571	0.4474
	25	0.5608	0.4517	0.5609	0.4518	0.5611	0.4520	0.5613	0.4524
0.15	0	0.5572	0.4469	0.5573	0.4471	0.5575	0.4473	0.5576	0.4475
	5	0.5592	0.4494	0.5593	0.4495	0.5595	0.4497	0.5596	0.4499
	10	0.5612	0.4519	0.5613	0.4521	0.5615	0.4523	0.5616	0.4526
	15	0.5632	0.4544	0.5633	0.4546	0.5635	0.4547	0.5636	0.4548
	25	0.5672	0.4592	0.5673	0.4593	0.5675	0.4595	0.5676	0.4596

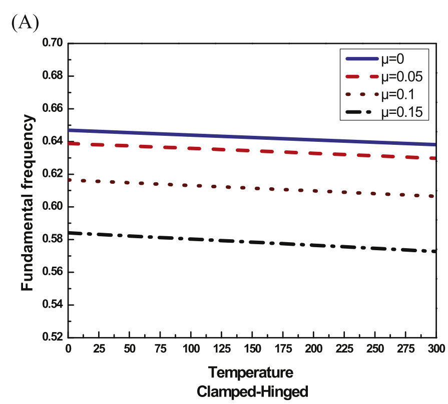

Fig. 2. Variation of fundamental frequency with temperature(ΔT °c), nonlocal parameter (μ) and different boundary conditions (A) Clamped-Hinged; and (B) Hinged-Hinged for elasticity supported piezoelectric nanobeam ($V_0 = 0$, L/h = 6, $k_1 = 25$, $k_2 = 0.05$, $k_3 = 0.025$).

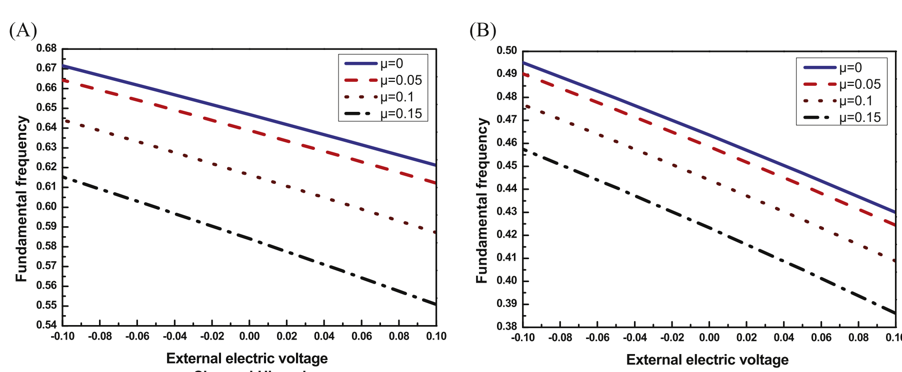

Fig. 3. Variation of fundamental frequency with external electric voltage V_0, nonlocal parameter (μ) and different boundary conditions (A) Clamped-Hinged; and (B) Hinged-Hinged for elasticity supported piezoelectric nanobeam.($\Delta T = 0$, L/h = 6, $k_1 = 25$, $k_2 = 0.05$, $k_3 = 0.025$)

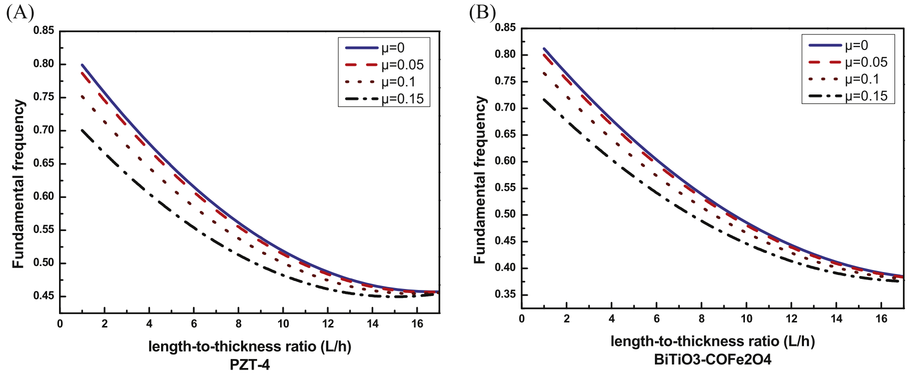

Fig. 4. Variation of fundamental frequency with length-to-thickness ratio (L/h), nonlocal parameter (μ) and different materials (A) PZT-4; and (B) BiTiO3–COFe2O4 for hinged elasticity supported piezoelectric nanobeam. ($V_0 = 0,\ \Delta T = 0,\ k_1 = 25,\ k_2 = 0.05,\ k_3 = 0.025$)

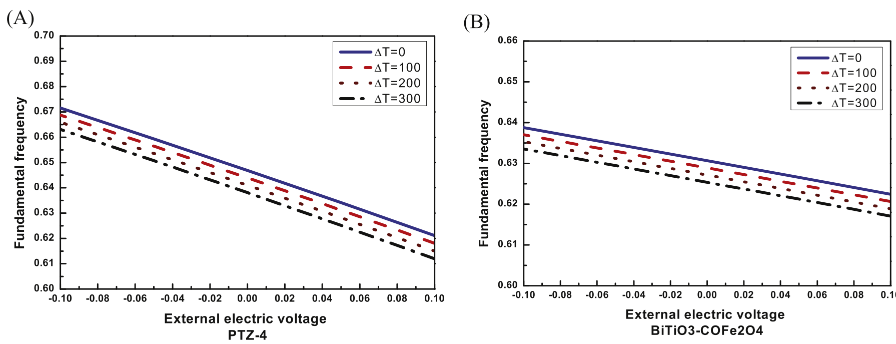

Fig. 5. Variation of fundamental frequency with external electric voltage V_0, temperature $\Delta T\ ^{\circ}c$ and different materials (A) PZT-4; and (B) BiTiO3–COFe2O4 for hinged elasticity supported piezoelectric nanobeam. ($L/h = 6,\ \mu = 0,\ k_1 = 25,\ k_2 = 0.05,\ k_3 = 0.025$)

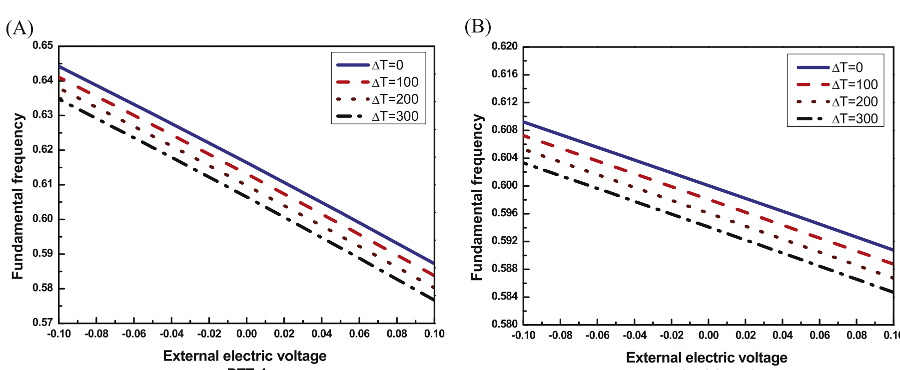

Fig. 6. Variation of fundamental frequency with external electric voltage V_0, temperature $\Delta T\ ^{\circ}c$ and different materials (A) PZT-4; and (B) BiTiO3–COFe2O4 for hinged elasticity supported piezoelectric nanobeam. ($L/h = 6,\ \mu = 0.1,\ k_1 = 25,\ k_2 = 0.05,\ k_3 = 0.025$)

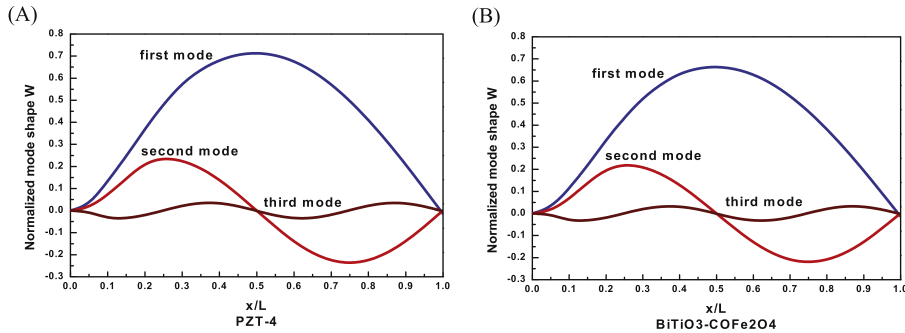

Fig. 7. Variation of normalized mode shape W with length of nanobeam for first three modes at different materials (A) PZT-4; and (B) BiTiO3–COFe2O4 for clamped hinged nanobeam. ($V_0 = 0$, $\Delta T = 100$, $L/h = 6$, $\mu = 0.1$, $k_1 = k_2 = k_3 = 0$)

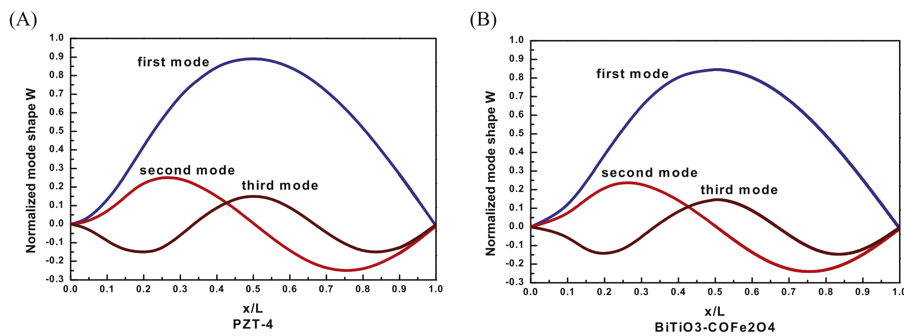

Fig. 8. Variation of normalized mode shape W with length of nanobeam for first three modes at different materials (A) PZT-4; and (B) BiTiO3–COFe2O4 for clamped hinged nanobeam resting on linear elastic foundation. ($V_0 = 0$, $\Delta T = 100$, $L/h = 6$, $\mu = 0.1$, $k_1 = 25$, $k_2 = 0.15$, $k_3 = 0$)

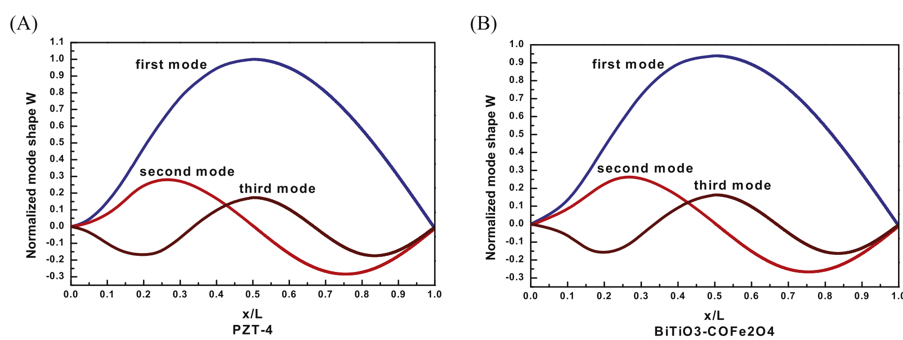

Fig. 9. Variation of normalized mode shape W with length of nanobeam for first three modes at different materials (A) PZT-4; and (B) BiTiO3–COFe2O4 for clamped hinged nanobeam resting on nonlinear elastic foundation. ($V_0 = 0$, $\Delta T = 100$, $L/h = 6$, $\mu = 0.1$, $k_1 = 25$, $k_2 = 0.15$, $k_3 = 0.5$)

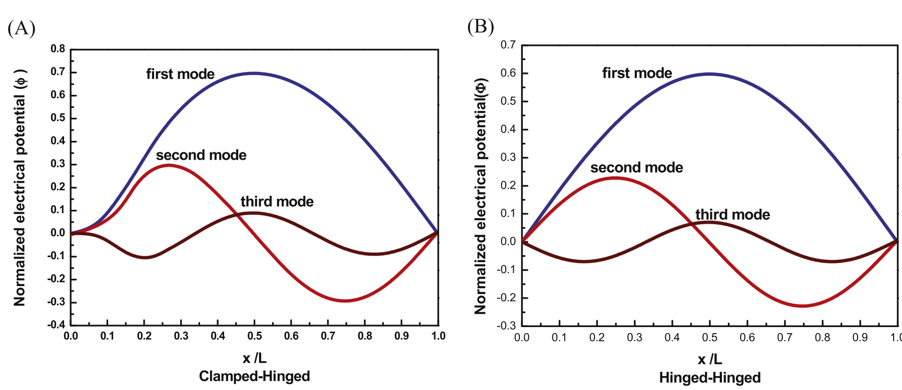

Fig. 10. Variation of normalized electrical potential (ϕ) with length of nanobeam for first three modes at BiTiO3–COFe2O4 Material for nanobeam (A) Clamped-Hinged; and (B) Hinged-Hinged. ($V_0 = 0$, $\Delta T = 100$, $L/h = 6$, $\mu = 0.1$, $k_1 = k_2 = k_3 = 0$)

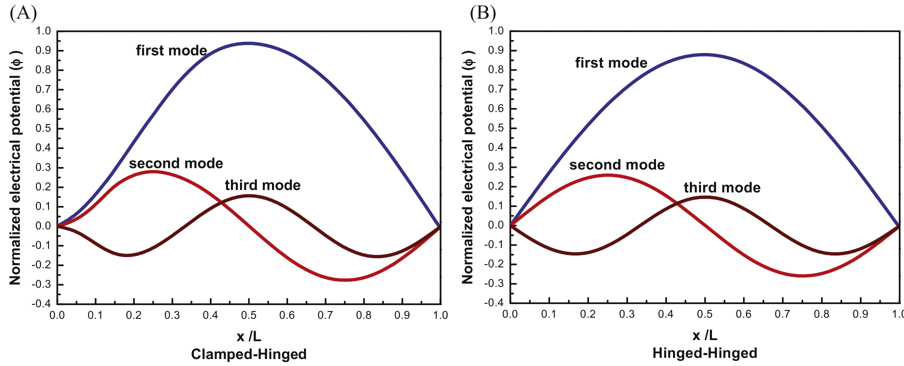

Fig. 11. Variation of normalized electrical potential (ϕ) with length of nanobeam for first three modes at BiTiO3–COFe2O4 Material for nanobeam resting on linear and nonlinear elastic foundation (A) Clamped-Hinged; and (B) Hinged-Hinged. ($V_0 = 0$, $\Delta T = 100$, $L/h = 6$, $\mu = 0.1$, $k_1 = 25$, $k_2 = 0.15$, $k_3 = 0$)

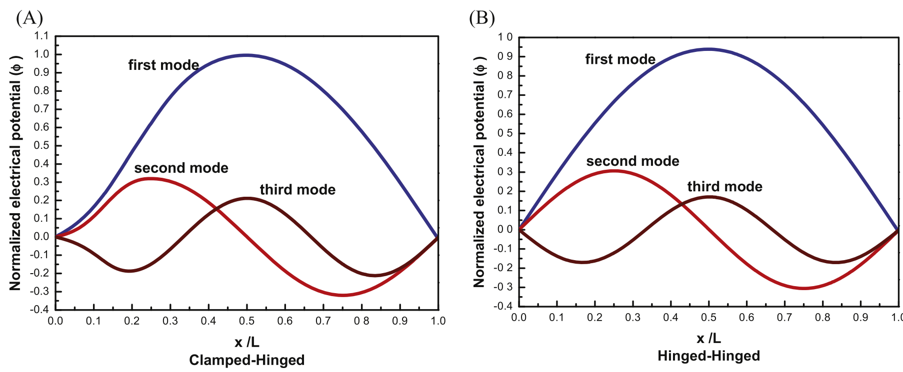

Fig. 12. Variation of normalized electrical potential (ϕ) with length of nanobeam for first three modes at BiTiO3–COFe2O4 material for nanobeam resting on linear and nonlinear elastic foundation (A) Clamped-Hinged; and (B) Hinged-Hinged. ($V_0 = 0$, $\Delta T = 100$, $L/h = 6$, $\mu = 0.1$, $k_1 = 25$, $k_2 = 0.15$, $k_3 = 0.15$)

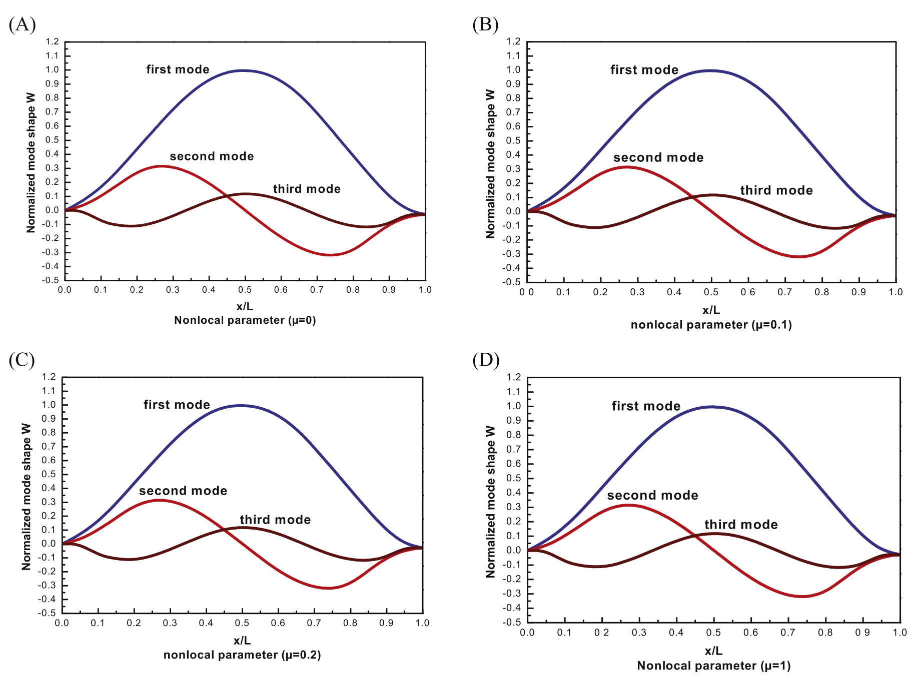

Fig. 13. Variation of normalized mode shape W with length of nanobeam for first three modes and nonlocal parameter (μ) (A) μ = 0 (B) μ = 0.1 (C) μ = 0.2; and (D) μ = 1 for clamped-clamped nanobeam resting on nonlinear elastic foundation. ($V_0 = 0$, $\Delta T = 100$, $L/h = 6$, $k_1 = 25$, $k_2 = 0.15$, $k_3 = 0.5$)

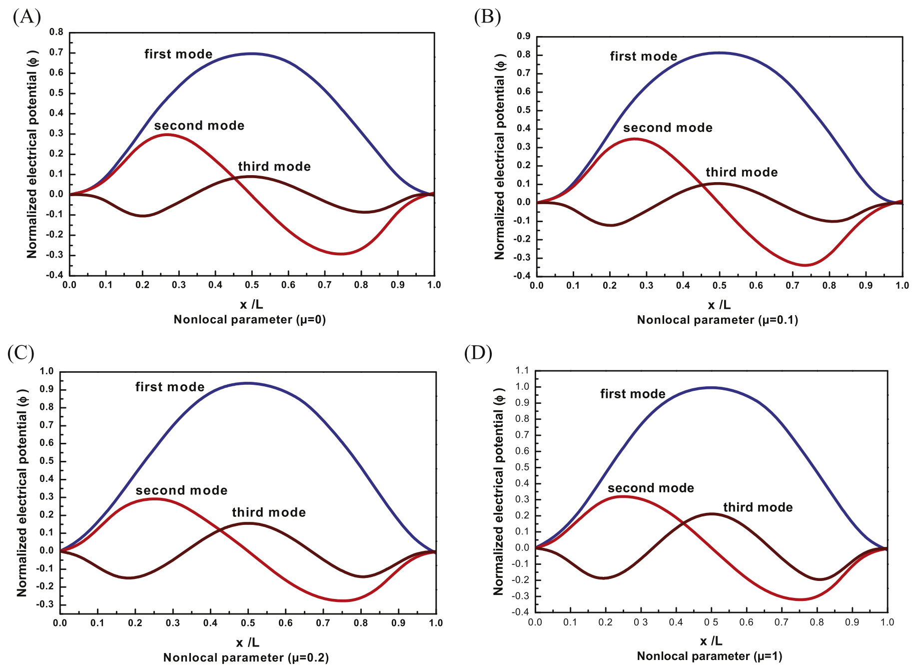

Fig. 14. Variation of normalized electrical potential (ϕ) with length of nanobeam for first three modes at PZT-4 material and nonlocal parameter (μ) (A) μ = 0 (B) μ = 0.1 (C) μ = 0.2; and (D) μ = 1 for clamped-clamped nanobeam resting on nonlinear elastic foundation. ($V_0 = 0$, $\Delta T = 100$, $L/h = 6$, $k_1 = 25$, $k_2 = 0.15$, $k_3 = 0.15$)

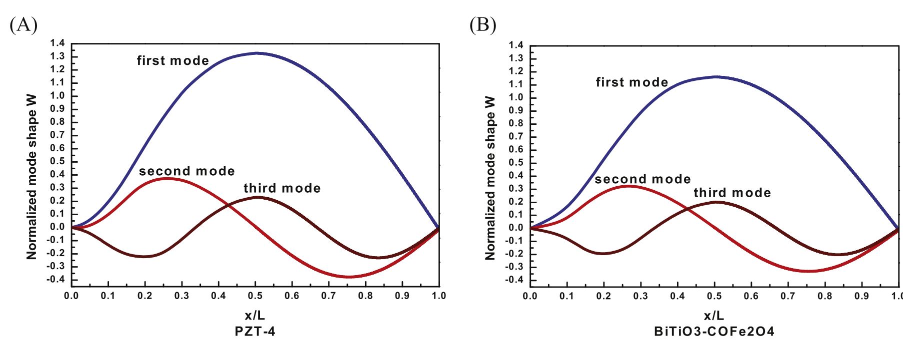

Fig. 15. Variation of normalized mode shape W with length of nanobeam for first three modes at different materials (A) PZT-4; and (B) BiTiO3–COFe2O4 for clamped hinged and open circuit nanobeam resting on nonlinear elastic foundation. ($V_0 = 0$, $\Delta T = 100$, $L/h = 6$, $\mu = 0.1$, $k_1 = 25$, $k_2 = 0.15$, $k_3 = 0.5$)

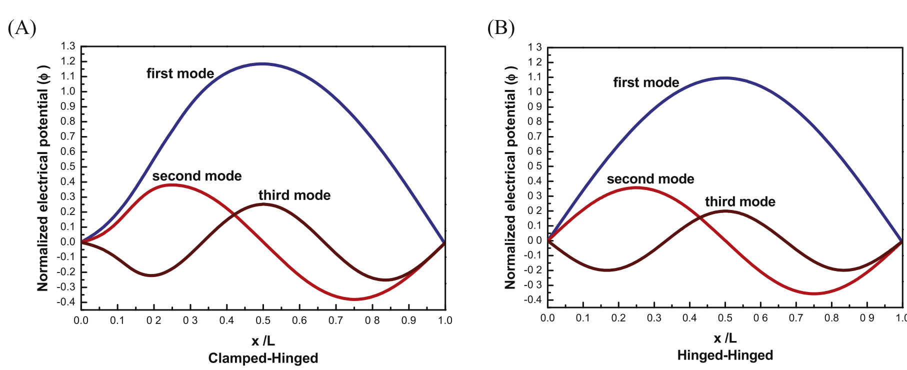

Fig. 16. Variation of normalized electrical potential (ϕ) with length of nanobeam for first three modes at BiTiO3–COFe2O4 material for open circuit nanobeam resting on linear and nonlinear elastic foundation (A) Clamped-Hinged; and (B) Hinged-Hinged.($V_0 = 0$, $\Delta T = 100$, $L/h = 6$, $\mu = 0.1$, $k_1 = 25$, $k_2 = 0.15$, $k_3 = 0.15$)

$$\frac{\partial v}{\partial x}|x=x_i=\sum_{j=-M}^{M}C_{ij}^{(1)}v(x_j),\frac{\partial^2 v}{\partial x^2}|x=x_i=\sum_{j=-M}^{M}C_{ij}^{(2)}v(x_j),$$
$$\frac{\partial^3 v}{\partial x^3}|x=x_i=\sum_{j=-M}^{M}C_{ij}^{(3)}v(x_j),\frac{\partial^4 v}{\partial x^4}|x=x_i=\sum_{j=-M}^{M}C_{ij}^{(4)}v(x_j),(i=-N,N), \tag{46}$$

Where σ is regularization parameter and r is a computational parameter. The weighting coefficients$C_{ij}^{(1)}$, $C_{ij}^{(2)}$, $C_{ij}^{(3)}$ *and* $C_{ij}^{(4)}$ can be defined as [57]:

$$C_{ij}^{(1)}=\begin{cases}\dfrac{(-1)^{i-j}}{h_x(i-j)}e^{-h_x^2\left(\frac{(i-j)^2}{2\sigma^2}\right)}, & i\neq j\\ 0 & i=j\end{cases},\ C_{ij}^{(2)}=\begin{cases}\left(\dfrac{2(-1)^{i-j+1}}{h_x^2(i-j)^2}+\dfrac{1}{\sigma^2}\right)e^{-h_x^2\left(\frac{(i-j)^2}{2\sigma^2}\right)}, & i\neq j\\ -\dfrac{1}{\sigma^2}-\dfrac{\pi^2}{3h_x^2} & i=j\end{cases}$$

$$C_{ij}^{(3)}=\begin{cases}\dfrac{(-1)^{i-j}}{h_x^3(i-j)^3}\left(\dfrac{\pi^2}{h_x^3(i-j)}+\dfrac{6}{h_x^3(i-j)^3}+\dfrac{3}{h_x(i-j)\sigma^2}+\dfrac{3h_x(i-j)}{\sigma^4}\right)e^{-h_x^2\left(\frac{(i-j)^2}{2\sigma^2}\right)}, & i\neq j\\ 0 & i=j\end{cases} \tag{47}$$

$$C_{ij}^{(4)}=\begin{cases}(-1)^{i-j}\left(\dfrac{4\pi^2}{h_x^4(i-j)^2}+\dfrac{4\pi^2}{h_x^2\sigma^2}-\dfrac{24}{h_x^4(i-j)^4}-\dfrac{12}{h_x^2(i-j)^2\sigma^2}-\dfrac{4h_x^2(i-j)^2}{\sigma^6}\right)e^{-h_x^2\left(\frac{(i-j)^2}{2\sigma^2}\right)}, & i\neq j\\ \dfrac{3}{\sigma^4}+\dfrac{2\pi^2}{h_x^2\sigma^2}+\dfrac{\pi^4}{5h_x^4} & i=j\end{cases}$$

On suitable substitution from (32,33,34,35,36,37,38,38,40,41,42,43,44,45,46,47) into (23,24,25,26), the problem can be reduced to the following Eigen-value problem:

$$\sum_{j=1}^{N}C_{ij}^{(2)}u_j=-\omega^2\left[\sum_{j=1}^{N}\delta_{ij}u_j-\mu^2\sum_{j=1}^{N}C_{ij}^{(2)}u_j\right], \tag{48}$$

$$\mathrm{k_s}\overline{\mathrm{A}}_{44}\left[\sum_{j=1}^{N}C_{ij}^{(2)}w_j+\eta\sum_{j=1}^{N}C_{ij}^{(1)}\psi_j\right]-\mathrm{k_s}\overline{\mathrm{E}}_{15}\sum_{j=1}^{N}C_{ij}^{(2)}\varphi_j+(\overline{\mathrm{N}}_\mathrm{E}+\overline{\mathrm{N}}_\mathrm{T})\sum_{j=1}^{N}C_{ij}^{(2)}w_j-(\overline{\mathrm{N}}_\mathrm{E}+\overline{\mathrm{N}}_\mathrm{T})\mu^2\sum_{j=1}^{N}C_{ij}^{(4)}w_j+$$
$$k_1\sum_{j=1}^{N}\delta_{ij}w_j-k_2\sum_{j=1}^{N}C_{ij}^{(2)}w_j+k_3\sum_{j=1}^{N}\delta_{ij}w_j^3=-\omega^2\left[\sum_{j=1}^{N}\delta_{ij}w_j-\mu^2\sum_{j=1}^{N}C_{ij}^{(2)}w_j\right], \tag{49}$$

$$\overline{\mathrm{D}}_{11}\sum_{j=1}^{N}C_{ij}^{(2)}\psi_j-\mathrm{k_s}\overline{\mathrm{A}}_{44}\eta\left(\sum_{j=1}^{N}C_{ij}^{(1)}w_j+\eta\sum_{j=1}^{N}\delta_{ij}\psi_j\right)+(\overline{\mathrm{F}}_{31}$$
$$+\mathrm{k_s}\overline{\mathrm{E}}_{15})\eta\sum_{j=1}^{N}C_{ij}^{(1)}\varphi_j$$
$$=-\overline{\mathrm{I}}_3\omega^2\left[\sum_{j=1}^{N}\delta_{ij}\psi_j-\mu^2\sum_{j=1}^{N}C_{ij}^{(2)}\psi_j\right], \tag{50}$$

$$\overline{\mathrm{F}}_{31}\eta\sum_{j=1}^{N}C_{ij}^{(1)}\psi_j+\overline{\mathrm{E}}_{15}\left[\sum_{j=1}^{N}C_{ij}^{(2)}w_j+\eta\sum_{j=1}^{N}C_{ij}^{(1)}\psi_j\right]+\overline{\mathrm{X}}_{11}\sum_{j=1}^{N}C_{ij}^{(2)}\varphi_j$$
$$-\overline{\mathrm{X}}_{33}\eta^2\sum_{j=1}^{N}\delta_{ij}\varphi_j$$
$$=0 \tag{51}$$

The boundary conditions (27–31) can also be approximated using three DQMs as:

(1) For Clamped - Clamped Beam (C–C)

$$\mathrm{u}_1=w_1=\psi_1=\varphi_1=0,\ \ at\ \zeta=0, \tag{52}$$

$$\mathrm{u}_N=w_N=\psi_N=\varphi_N=0,\ \ at\ \zeta=1, \tag{53}$$

(2) For Hinged- Hinged Beam (H–H):

$$\overline{\mathrm{F}}_{31}\eta\sum_{j=1}^{N}\delta_{1j}\varphi_j-\mu^2\omega^2\left[\overline{I}_3\sum_{j=1}^{N}C_{1j}^{(2)}\psi_j+\eta\sum_{j=1}^{N}\delta_{1j}wj-\mu^2\eta\sum_{j=1}^{N}C_{1j}^{(2)}u_j\right]-(\overline{\mathrm{N}}_{\mathrm{T}}+\overline{\mathrm{N}}_{\mathrm{E}})\eta\sum_{j=1}^{\mathrm{N}}\mathrm{C}_{1j}^{(2)}\mathrm{w}_j=0, \quad u_1=w_1=\varphi_1=0 \quad \text{at } \zeta=0 \tag{54}$$

$$\overline{\mathrm{F}}_{31}\eta\sum_{j=1}^{N}\delta_{Nj}\varphi_j-\mu^2\omega^2\left[\overline{I}_3\sum_{j=1}^{N}C_{Nj}^{(2)}\psi_j+\eta\sum_{j=1}^{N}\delta_{Nj}wj-\mu^2\eta\sum_{j=1}^{N}C_{Nj}^{(2)}u_j\right]-(\overline{\mathrm{N}}_{\mathrm{T}}+\overline{\mathrm{N}}_{\mathrm{E}})\eta\sum_{j=1}^{\mathrm{N}}\mathrm{C}_{Nj}^{(2)}\mathrm{w}_j=0, \quad \mathrm{u}_N=w_{\mathrm{N}}=\varphi_N=0 \quad \text{at } \zeta=1 \tag{55}$$

(3) For Clamped - Hinged Beam (C–H):

$$\mathrm{u}_1=w_1=\psi_1=\varphi_1=0, \quad at\ \zeta=0, \tag{56}$$

$$\overline{\mathrm{F}}_{31}\eta\sum_{j=1}^{N}\delta_{Nj}\varphi_j-\mu^2\omega^2\left[\sum_{j=1}^{N}C_{Nj}^{(2)}\psi_j+\eta\sum_{j=1}^{N}\delta_{Nj}wj-\mu^2\eta\sum_{j=1}^{N}C_{Nj}^{(2)}u_j\right]-(\overline{\mathrm{N}}_{\mathrm{T}}+\overline{\mathrm{N}}_{\mathrm{E}})\eta\sum_{j=1}^{\mathrm{N}}\mathrm{C}_{Nj}^{(2)}\mathrm{w}_j=0, \quad \mathrm{u}_N=w_{\mathrm{N}}=\varphi_N=0 \quad \text{at } \zeta=1 \tag{57}$$

For closed circuit:

$$\varphi_1=0 \ \text{at}\ \zeta=0,\ \varphi_N=0 \ \text{at}\ \zeta=1, \tag{58}$$

For open circuit

$$\begin{aligned}\overline{F}_{31}\eta\sum_{j=1}^{N}C_{1j}^{(1)}\psi-\overline{X}_{33}\eta^2\sum_{j=1}^{N}\delta_{1j}\varphi_j=0 \ \text{at}\ \zeta=0\\ \overline{F}_{31}\eta\sum_{j=1}^{N}C_{Nj}^{(1)}\psi-\overline{X}_{33}\eta^2\sum_{j=1}^{N}\delta_{Nj}\varphi_j=0 \ \text{at}\ \zeta=1\end{aligned} \tag{59}$$

4. Results & discussion

The present numerical results demonstrate the convergence and efficiency of each one of the proposed schemes for vibration analysis of piezoelectric nanobeam resting on nonlinear elastic foundation. This beam is made of PZT-4 and BiTiO3–COFe2O4. For all results, the boundary conditions (52–59) are augmented in the governing Eqs. (48), (49), (50), and (51). After that using iterative quadrature technique to solve this problem. The computational characteristics of each scheme are adapted to reach accurate results with error of order $\leq 10^{-10}$. The obtained frequencies ω can be evaluated such as:

$$\omega=\Omega L\sqrt{\frac{\mathrm{I}_1}{\mathrm{A}_{11}}} \quad \text{where } \Omega \text{ is the natural frequency of piezoelectric nanobeam} \tag{60}$$

For the present results, material parameters are taken from the macroscopic piezoelectric material. These materials are listed in Table 1.

For PDQM the problem is solved over a non-uniform grids, with Gauss – Chebyshev – Lobatto discretizations, such as [56]:

$$x_i=\frac{1}{2}\left[1-\cos\left(\frac{i-1}{N-1}\pi\right)\right], (i=1:N) \tag{61}$$

Where the dimensions of the grid (N) ranges from 3 to 15.

The obtained results agreed with previous analytical ones [59] over 7 grid sizes, shown in Table 2.

For SincDQ scheme, the problem is solved over regular grids ranging from 3 to 15. Table 3 shows the convergence of the obtained results. They agreed with exact ones [59] over grid size ≥ 9. Also, this table shows that the execution time of SincDQ scheme is less than that of PDQM. Therefor, it is more efficient than PDQM for vibration analysis of nanobeam.

For DSCDQ scheme based on delta Lagrange kernel, the problem is also solved over a uniform grid ranging from 3 to 11. The bandwidth 2M + 1 ranges from 3 to 11. Table 4 shows the convergence of the obtained fundamental frequency which agreed with exact ones [60] over grid size ≥ 3 and bandwidth ≥ 3. Tables 4,5 show that the execution time of DSCDQM-DLK is less than that of PDQM and SincDQM.

For DSCDQ scheme based on regularized Shannon kernel (RSK), the problem is also solved over a uniform grid ranging from 3 to 15. The bandwidth 2M + 1 ranges from 3 to 9 and the regularization parameter $\sigma = r\ h_x$ ranges from $1h_x$ to $2\ h_x$, where $h_x = 1/N\text{-}1$. Table 6 shows the convergence of the obtained fundamental frequency to the exact and numerical ones [19,60] over grid size ≥ 3, bandwidth ≥ 3 and regulization parameter $\sigma = 2\ h_x$. Table 7 also ensures that the execution time of this scheme is the least. Therefore, the DSCDQM-RSK scheme is the best choice among the examined quadrature schemes for vibration analysis of piezoelectric nanobeam resting on the nonlinear elastic foundation.

Furthermore, a parametric study is introduced to investigate the influence of linear and nonlinear elastic foundations parameters, temperature change($\Delta T\ ^\circ C$), external electric voltage (V_0), nonlocal parameter (μ), length-to-thickness ratio (L/h), different boundary conditions and different materials on the values of natural frequencies and mode shapes. But, the parametric study is introduced over grid 3 nodes, bandwidth ≥ 3 and regulization parameter $\sigma = 2\ h_x$ by DSCDQM-RSK scheme.

Tables 8,9,10,11 show that the natural frequency increases with increasing linear elastic foundation parameters. Also, the computations declare that the natural frequencies do not affect significantly by nonlinear elastic foundation parameter k_3. Tables 10 and 11 show that the natural frequencies decrease with increasing nonlocal parameter (μ) and length-to-thickness ratio (L/h) at different conditions of linear and nonlinear parameters of elastic foundation. But, an exact value is not known for the nonlocal parameter (μ) on the vibration behaviour of elasticity supported piezoelectric nanobeam, we assumed a range of values $0 \leq \mu \leq 1$. Table (10) shows that the value of nonlocal parameter $0 \leq \mu \leq 0.2$ agrees with the experimental findings of a smaller is stiffer, size effect [16,17,18,19] ($\mu = 0$ mean that the nanobeam is the classical without the nonlocal effect). Also, the values of natural frequencies depending on the boundary conditions. Furthermore, the change of the value of natural frequencies not significant when L/h ≥16. As well, it can be seen that for all boundary conditions the nonlocal parameter has a more effect for higher frequency than lower one. Furthermore, for all boundary conditions the length-to-thickness ratio decreasing the all-natural frequencies are the same. Tables 12,13,14 show that the natural frequencies for an open circuit are higher than short circuit boundary conditions. For all tables the nanobeam made of PZT-4.

Figs. 2, 3, 4, 5, and 6 show that the fundamental frequency decrease with increasing temperature change($\Delta T\ ^\circ C$), external electric voltage V_0, nonlocal parameter (μ) and length-to-thickness ratio (L/h). From Fig. (4), the change of the value of natural frequencies not significant when L/h ≥16. It is mean that the increase in length-to-thickness ratio of the piezoelectric nanobeam decreases the nonlocal effects and the nonlocal curve converges with local theory results ($\mu = 0$). Furthermore, the type of the materials made of nanobeam is influenced by temperature change, external electric voltage, nonlocal parameter and length-to-thickness ratio (L/h). So, the fundamental frequency W for PZT-4 material is higher than BiTiO3–COFe2O4 material.

As well as, Figs. 7, 8, 9, 10, 11, 12, 13, and 14 show the first three normalized mode shapes W and electrical potential ϕ with length of nanobeam $\zeta = \frac{x}{L}$at different materials, linear and nonlinear parameters of elastic foundation and boundary conditions. Figs. 7, 8, 9, 10, 11, 12, 13, and 14 were normalized by the corresponding maximum value in magnitude for W (0.5) and $\phi(0.5)$ at $(k_1 = 25, k_2 = 0.15, k_3 = 0.5)$. These figures show that the amplitudes of displacement W and electrical potential ϕincrease with increasing linear and nonlinear elastic foundation parameters. Furthermore, these figures show that the normalized amplitude W and electrical potential ϕ for PZT-4 material is higher than BiTiO3–COFe2O4 material. Also, Figs.13 and 14 show that the nonlocal parameter (μ) not effect on the normalized amplitude W but has an effect on the normalized electrical potential ϕ. Figs. 15 and 16 explain that open circuit boundary conditions change strongly the modal shapes. By comparing the natural frequencies and modal shapes for each case, it is also found that the boundary conditions play a critical role in determining the natural frequencies and modal shapes. Also, it is found that the nanobeam is insensitive to the temperature change while the external electric potential has the greatest effect on the natural frequencies. Fundamental frequencies depend on the sign and magnitude of the external electric potential. Furthermore, the best value of nonlocal parameter (μ) on the vibration behaviour of elasticity supported piezoelectric nanobeam is $0 \leq \mu \leq 0.2$.

5. Conclusion

Three Different Quadrature schemes (PDQM, SDQM,DSCDQM-DLK, DSCDQM-RSK), have been successfully applied for free vibration analysis of piezoelectric nanobeam resting on linear and nonlinear elastic foundation. Also, we are using an iterative quadrature technique to solve the reduced system. MATLAB program is designed for each scheme such that the maximum error (comparing with the previous exact results) is $\leq 10^{-10}$. Also, Execution time for each scheme, is determined. It is concluded that discrete singular convolution differential quadrature method based on regularized Shannon kernel (DSCDQM-RSK) with grid size ≥ 3, bandwidth 2M + 1 ≥ 3 and regulization parameter $\sigma = 2{*}h_x$ leads to best accurate efficient results for the concerned problem. Based on this scheme, a parametric study is introduced to investigate the influence of linear and nonlinear elastic foundation, geometric characteristics and type of material of the vibrated beam, on results. For all results, it is found that:

- Natural frequencies increase with increasing linear elastic foundation parameters.
- Fundamental frequency decrease with increasing temperature change ($\Delta T\ ^\circ$c), external electric voltage V_0, nonlocal parameter (μ) and length-to-thickness ratio (L/h).
- Amplitudes of displacement W and electrical potential ϕ increase with increasing linear and nonlinear elastic foundation parameters.
- Fundamental frequency, normalized amplitude W and electrical potential ϕ for PTZ-4 material are higher than BiTiO3–COFe2O4 material.
- Natural frequencies of C–C is heigher than the other boundary conditions.
- The change of the value of natural frequencies not significant when L/h ≥16.
- Increase in length-to-thickness ratio of the piezoelectric nanobeam decreases the nonlocal effects and the nonlocal curve converges with local theory results ($\mu = 0$).
- The best value of nonlocal parameter (μ) on the vibration behavior of elasticity supported piezoelectric nanobeam is $0 \leq \mu \leq 0.2$.
- The natural frequencies, normalized amplitude W and electrical potential (∅) for open circuit is higher than short circuit.

It is aimed that these results may be useful for design purpose, electromechanical applications and many fields of the industrial revolution. The most important applications of nanobeam are likely to take advantage of their exceptional mechanical, chemical and electrical properties to be used as sensors, resonators and transducers for nanoelectronic and biotechnology applications.

Declarations

Author contribution statement

Ola Ragb: Analyzed and interpreted the data; Contributed reagents, materials, analysis tools or data; Wrote the paper.

Mokhtar Mohamed: Conceived and designed the experiments; Performed the experiments; Wrote the paper.

Mohamed S. Matbuly: Analyzed and interpreted the data.

Funding statement

This research did not receive any specific grant from funding agencies in the public, commercial, or not-for-profit sectors.

Competing interest statement

The authors declare no conflict of interest.

Additional information

No additional information is available for this paper.

References

[1] F. Ebrahimi, M. Zia, Large amplitude nonlinear vibration analysis of functionally graded Timoshenko beams with porosities, Acta Astronaut. 116 (2015) 117–125.
[2] F. Ebrahimi, F. Ghasemi, E. Salari, Investigating thermal effects on vibration behavior of temperature-dependent compositionally graded Euler beams with porosities, Meccanica 51 (2016) 223–249.
[3] F. Ebrahimi, E. Salari, Size-dependent thermo-electrical buckling analysis of functionally graded piezoelectric nanobeams, Smart Mater. Struct. 24 (2015) 125007.
[4] F. Ebrahimi, A. Rastgoo, M. Kargarnovin, Analytical investigation on axisymmetric free vibrations of moderately thick circular functionally graded plate integrated with piezoelectric layers, J. Mech. Sci. Technol. 22 (2008) 1058–1072.
[5] F. Ebrahimi, M. Mokhtari, Transverse vibration analysis of rotating porous beam with functionally graded microstructure using the differential transform method, J. Braz. Soc. Mech. Sci. Eng. 37 (2015) 1435–1444.

[6] X.-F. Li, G.-J. Tang, Z.-B. Shen, K.Y. Lee, Resonance frequency and mass identification of zeptogram-scale nanosensor based on the nonlocal beam theory, Ultrasonics 55 (2015) 75–84.
[7] S. Xu, Z. Wang, One-dimensional ZnO nanostructures: solution growth and functional properties, Nano Res 4 (2011) 1013–1098.
[8] Z. Wang, ZnO, nanowire and nanobelt platform for nanotechnology Mater, Sci. Eng. R 64 (2009) 33–71.
[9] L. Ke, Y.S. Wang, W. Zheng-Dao, Nonlinear vibration of the piezoelectric nanobeams based on the nonlocal theory, Compos. Struct. 94 (2012) 2038–2047.
[10] F. Ebrahimi, M.F. Barati, Modeling of smart magnetically affected flexoelectric/piezoelectric nanostructures incorporating surface effects, Nanomater. Nanotechnol. 7 (2017) 1–11.
[11] W.J. Chen, X.P. Li, Size-dependent free vibration analysis of composite laminated Timoshenko beam based on new modified couple stress theory, Arch. Appl. Mech. 83 (2012) 431–444.
[12] Z.-B. Shen, L.-P. Sheng, X.-F. Li, G.-J. Tang, Nonlocal Timoshenko beam theory for vibration of carbon nanotube-based biosensor, Physica 44 (2012) 1169–1176.
[13] Z.-B. Shen, X.-F. Li, L.-P. Sheng, G.-J. Tang, Transverse vibration of nanotube-based micro-mass sensor via nonlocal Timoshenko beam theory, Comput. Mater. Sci. 53 (2012) 340–346.
[14] X.F. Li, B.L. Wang, Vibrational modes of Timoshenko beams at small scales, Appl. Phys. Lett. 94 (2009) 101903.
[15] Y. Huang, Q.Z. Luo, X.F. Li, Transverse waves propagating in carbon nanotubes via a higher-order nonlocal beam model, Compos. Struct. 95 (2013) 328–336.
[16] B. Akgöz, O. Civalek, Buckling analysis of cantilever carbon nanotubes using the strain gradient elasticity and modified couple stress theories, J. Comput. Theor. Nanosci. 8 (2011) 1821–1827.
[17] C. Li, A nonlocal analytical approach for torsion of cylindrical nanostructures and the existence of higher-order stress and geometric boundaries, Compos. Struct. 118 (2014) 607–621.
[18] J.P. Shen, C. Li, A semi-continuum-based bending analysis for extreme-thin micro/nano-beams and new proposal for nonlocal differential constitution, Compos. Struct. 172 (2017) 210–220.
[19] K. Mercan, O. Civalek, DSC method for buckling analysis of boron nitride nanotube (BNNT) surrounded by an elastic matrix, Compos. Struct. 143 (2016) 300–309.
[20] A. Lazarus, O. Thomas, J.-F. Deü, Finite element reduced order models for nonlinear vibrations of piezoelectric layered beams with applications to NEMS, Finite Elem. Anal. Des. 49 (2012) 35–51.
[21] S.M. Tanner, J.M. Gray, C.T. Rogers, K.A. Bertness, N.A. Sanford, High-Q GaN nanowire resonators and oscillators, Appl. Phys. Lett. 91 (2007) 203117.
[22] Q. Wang, Q.H. Li, Y.J. Chen, T.H. Wang, X.L. He, J.P. Li, Fabrication and ethanol sensing characteristics of ZnO nanowire gas sensors, Appl. Phys. Lett. 84 (2004) 3654–3656.
[23] M. Şimşek, H. Yurtcu, Analytical solutions for bending and buckling of functionally graded nanobeams based on the nonlocal Timoshenko beam theory, Compos Struct. 97 (2013) 378–386.
[24] A.A. Jandaghian, O. Rahmani, An analytical solution for free vibration of piezoelectric nanobeams based on a nonlocal elasticity theory, Journal of Mechanics 32 (2016) 143–151.
[25] A.A. Jandaghian, A.A. Jafari, O. Rahmani, Exact solution for Transient bending of a circular plate integrated with piezoelectric layers, Appl. Math. Model. 37 (2013) 7154–7163.
[26] A. Norouzzadeh, R. Ansari, Finite element analysis of nano-scale Timoshenko beams using the integral model of nonlocal elasticity, Phys. Met. 88 (2017) 194–200.
[27] F. Tornabene, N. Fantuzzi, F. Ubertini, E. Viola, Strong formulation finite element method based on differential quadrature: a survey, Appl. Mech. Rev. 67 (2015), 020801.
[28] C.M.C. Roque, D.S. Fidalgo, A.J.M. Ferreira, J.N. Reddy, A study of a microstructure-dependent composite laminated Timoshenko beam using a modified couple stress theory and a meshless method, Compos. Struct. 96 (2013) 532–537.
[29] K. Abbas, H. Ali, F. Hamidreza, Free vibration analysis of a Piezoelectric nanobeam using nonlocal elasticit y theory, Struct. Eng. Mech. 61 (2017) 617–624.
[30] H. Foroughi, M. Azhari, Mechanical buckling and free vibration of thick functionally graded plates resting on elastic foundation using the higher order B-spline finite strip method, Meccanica 49 (2014) 981–993.
[31] W.J. Manning, A.R. Plummer, M.C. Levesley, Vibration control of a flexible beam with integrated actuators and sensors, Smart Mater. Struct. 9 (2000) 932–939.
[32] M. Fakher, H.H. Shahrokh, Bending and free vibration analysis of nano beams by differential and integral forms of nonlocal strain gradient with Rayleigh–Ritz method, Mater. Res. Express 4 (2017) 125025.
[33] G. Karami, P. Malekzadeh, A new differential quadrature methodology for beam analysis and the associated differential quadrature element method, Comput. Methods Appl. Mech. Eng. 191 (2002) 3509–3526.
[34] P. Malekzadeh, G. Karami, Polynomial and harmonic differential quadrature methods for free vibration of variable thickness thick shew plates, Eng. Struct. 27 (2005) 1563–1574.
[35] M.F. Shojaeim, R. Ansari, Variational differential quadrature: a technique to simplify numerical analysis of structures, Appl. Math. Model. 49 (2017) 705–738.
[36] F. Tornabene, E. Viola, D.J. Inman, 2-D differential quadrature solution for vibration analysis of functionally graded conical, cylindrical shell and annular plate structures, J. Sound Vib. 328 (2009) 259–290.
[37] F. Tornabene, N. Fantuzzi, E. Viola, E. Carrera, Static analysis of doubly-curved anisotropic shells and panels using CUF approach, differential geometry and differential quadrature method, Compos. Struct. 107 (2014) 675–697.
[38] F. Tornabene, R. Dimitri, E. Viola, Transient dynamic response of generally shaped arches based on a GDQ-Time-stepping method, Int. J. Mech. Sci. 114 (2016) 277–314.
[39] A. Korkmaz, D. İdris, Shock wave simulations using Sinc differential quadrature method, engineering computations, International Journal for Computer-Aided Engineering and Software 28 (2011) 654–674.
[40] O. Civalek, O. Kiracioglu, Free vibration analysis of Timoshenko beams by DSC method, Int. J. Numer. Meth. Biomed. Engng. 26 (2010) 250–275.
[41] M. Gürses, O. Civalek, A. Korkmaz, H. Ersoy, Free vibration analysis of symmetric laminated skew plates by discrete singular convolution technique based on first-order shear deformation theory, Int. J. Numer. Methods Eng. 79 (2009) 290–313.
[42] A.K. Baltacıoglu, B. Akgoz, O. Civalek, Nonlinear static response of laminated composite plates by discrete singular convolution method, Compos. Struct. 93 (2010) 153–161.
[43] A.K. Baltacıoglu, O. Civalek, B. Akgoz, F. Demir, Large deflection analysis of laminated composite plates resting on nonlinear elastic foundations by the method of discrete singular convolution, Int. J. Press. Vessel. Pip. 88 (2011) 290–300.
[44] A. Seçkin, A.S. Sarıgül, Free vibration analysis of symmetrically laminated thin composite plates by using discrete singular convolution (DSC) approach: algorithm and verification, J. Sound Vib. 315 (2009) 197–211.
[45] O. Civalek, The determination of frequencies of laminated conical shells via the discrete singular convolution method, J. Mech. Mater. Struct. 1 (2006) 163–182.
[46] O. Civalek, Vibration analysis of conical panels using the method of discrete singular convolution, Commun. Numer. Methods Eng. 24 (2008) 169–181.
[47] O. Civalek, Fundamental frequency of isotropic and orthotropic rectangular plates with linearly varying thickness by discrete singular convolution method, Appl. Math. Model. 33 (2009) 3825–3835.
[48] O. Civalek, B. Akgöz, Vibration analysis of micro-scaled sector shaped graphene surrounded by an elastic matrix, Comput. Mater. Sci. 77 (2013) 295–303.
[49] O. Civalek, Free vibration of carbon nanotubes reinforced (CNTR) and functionally graded shells and plates based on FSDT via discrete singular convolution method, Composites Part B 111 (2017) 45–59.
[50] C. Demir, K. Mercan, O. Civalek, Determination of critical buckling loads of isotropic, FGM and laminated truncated conical panel, Composites Part B 94 (2016) 1–10.
[51] G.W. Wei, Vibration analysis by discrete singular convolution, J. Sound Vib. 244 (2001) 535–553.
[52] A.A. Jandaghian, O. Rahmani, Free vibration analysis of magneto-electrothermo elastic nanobeams resting on a Pasternak foundation, Smart Mater. Struct. 25 (2016), 035023.
[53] B. Akgöz, O. Civalek, Nonlinear vibration analysis of laminated plates resting on nonlinear two-parameters elastic foundations, Steel Compos. Struct. 11 (2011) 403–421.
[54] O. Civalek, Nonlinear dynamic response of laminated plates resting on nonlinear elastic foundations by the discrete singular convolution-differential quadrature coupled approaches, Composites Part B 50 (2013) 171–179.
[55] G.C. Tsiatas, A new efficient method to evaluate exact stiffness and mass matrices of non-uniform beams resting on an elastic foundation, Arch. Appl. Mech. 84 (2014) 615–623.
[56] S. Chang, Differential Quadrature and its Application in Engineering, Springer-Verlag London Ltd., 2000.
[57] G.W. Wei, A new algorithm for solving some mechanical problems, Comput. Methods Appl. Mech. Eng. 190 (2001) 2017–2030.
[58] Q. Wang, Axi-symmetric wave propagation in a cylinder coated with a piezoelectric layer, Int. J. Solids Struct. 39 (2002) 3023–3037.
[59] R. Ansari, R. Gholami, H. Rouhi, Size-dependent nonlinear forced vibration analysis of magneto-electro-thermo-elastic Timoshenko nanobeams based upon the nonlocal elasticity theory, Compos. Struct. 126 (2015) 216–226.
[60] A.A. Jandaghian, O. Rahmani, An analytical solution for free vibration of piezoelectric nanobeams based on a nonlocal elasticity theory, Smart Mater. Struct. 32 (2016) 143–151.
[61] Y. Li, Z.F. Shi, Free vibration of a functionally graded piezoelectric beam via state-space based differential quadrature, Compos. Struct. 87 (2009) 257–264.